Sarcoplasmic Reticulum Lumenal Ca^{2+} Has Access to Cytosolic Activation and Inactivation Sites of Skeletal Muscle Ca^{2+} Release Channel

Ashutosh Tripathy and Gerhard Meissner
Departments of Biochemistry and Biophysics, and Physiology, University of North Carolina, Chapel Hill, North Carolina, 27599-7260 USA

ABSTRACT The effects of sarcoplasmic reticulum lumenal (*trans*) Ca^{2+} on cytosolic (*cis*) ATP-activated rabbit skeletal muscle Ca^{2+} release channels (ryanodine receptors) were examined using the planar lipid bilayer method. Single channels were recorded in symmetric 0.25 M KCl media with K^+ as the major current carrier. With nanomolar [Ca^{2+}] in both bilayer chambers, the addition of 2 mM cytosolic ATP greatly increased the number of short channel openings. As lumenal [Ca^{2+}] was increased from <0.1 μM to ~250 μM, increasing channel activities and events with long open time constants were seen at negative holding potentials. Channel activity remained low at positive holding potentials. Further increase in lumenal [Ca^{2+}] to 1, 5, and 10 mM resulted in a decrease in channel activities at negative holding potentials and increased activities at positive holding potentials. A voltage-dependent activation by 50 μM lumenal Ca^{2+} was also observed when the channel was minimally activated by <1 μM cytosolic Ca^{2+} in the absence of ATP. With μM cytosolic Ca^{2+} in the presence or absence of 2 mM ATP, single-channel activities showed no or only a weak voltage dependence. Other divalent cations (Mg^{2+}, Ba^{2+}) could not replace lumenal Ca^{2+}. On the contrary, cytosolic ATP-activated channel activities were decreased as lumenal Ca^{2+} fluxes were reduced by the addition of 1–5 mM $BaCl_2$ or $MgCl_2$ to the lumenal side, which contained 50 μM Ca^{2+}. An increase in [KCl] from 0.25 M to 1 M also reduced single-channel activities. Addition of the "fast" Ca^{2+} buffer 1,2-bis(2-aminophenoxy)ethanetetraacetic acid (BAPTA) to the *cis* chamber increased cytosolic ATP-, lumenal Ca^{2+}-activated channel activities to a nearly maximum level. These results suggested that lumenal Ca^{2+} flowing through the skeletal muscle Ca^{2+} release channel may regulate channel activity by having access to cytosolic Ca^{2+} activation and Ca^{2+} inactivation sites that are located in "BAPTA-inaccessible" and "BAPTA-accessible" spaces, respectively.

INTRODUCTION

In striated muscle, Ca^{2+} release from an intracellular membrane compartment, the sarcoplasmic reticulum (SR), is mediated by large protein structures commonly known as "feet," Ca^{2+} release channels, or ryanodine receptors (RyRs) (for a review, see Meissner, 1994). The RyR ion channel has been purified as a 30 S protein complex and shown to be composed of four large RyR polypeptides of ~5000 amino acid residues and four immunophilins (FK506 binding protein) of ~100 amino acid residues each. In vitro regulation of the RyR ion channel has been extensively investigated in Ca^{2+} flux–SR vesicle and [^{3}H]ryanodine binding measurements, and by recording single channel activities using the planar lipid bilayer method. These studies have shown that the skeletal muscle Ca^{2+} release channel is regulated by various endogenous effectors, including Ca^{2+}, Mg^{2+}, ATP, and calmodulin. Among these effectors, Ca^{2+} is of particular significance. Channel activity has been suggested to be affected by SR lumenal Ca^{2+} and to be regulated in a biomodal manner by cytosolic Ca^{2+}. At nanomolar cytosolic Ca^{2+}, the channel rarely opened in the absence of other channel activators. As the cytosolic [Ca^{2+}] was increased, channel activity increased, reaching a maximum at 10–50 μM Ca^{2+}, and then again fell close to zero as the cytosolic [Ca^{2+}] was increased to millimolar levels. Bimodal Ca^{2+} dependence of channel activity suggested that the Ca^{2+} release channel possesses high-affinity Ca^{2+} activation and low-affinity Ca^{2+} inactivation sites that are accessible from the cytosolic side and have been presumed to be located in the large cytosolic foot region of the channel (Meissner, 1994). There have been a limited number of studies describing the effects of lumenal Ca^{2+} on Ca^{2+} release channel activity. In vesicle-Ca^{2+} flux measurements, an increase in lumenal [Ca^{2+}] shifted the Ca^{2+} activation curve to lower [Ca^{2+}] (Meissner et al., 1986) and increased the rate constant of Ca^{2+} efflux from rabbit and frog skeletal muscle triads (Donoso et al., 1995). In single-channel measurements with rabbit and pig skeletal muscle release channels, an increase in lumenal Ca^{2+} from micromolar to millimolar levels decreased channel activity, suggesting that the cytosolic inactivating Ca^{2+} site was accessible from the lumenal side (Ma et al., 1988; Fill et al., 1990). In single-channel measurements with sheep skeletal muscle release channels, cytosolic ATP-activated and lumenal Ca^{2+}-dependent channel openings were observed; however, it was considered to be unlikely that this activation was due to lumenal Ca^{2+} gaining access to a cytosolic activating site (Sitsapesan and Williams, 1995).

In this study we have investigated the effects of different lumenal [Ca^{2+}] (from <0.1 μM to 10 mM) on Ca^{2+} release

Received for publication 18 September 1995 and in final form 27 February 1996.

Address reprint requests to Dr. Gerhard Meissner, Department of Biochemistry and Biophysics, University of North Carolina, CB 7260, Chapel Hill, NC 27599-7260. Tel.: 919-966-5021; Fax: 919-966-2852; E-mail: meissner@nun.oit.unc.edu.

0006-3495/96/06/2600/16 $2.00

channel activity at suboptimally activating levels of cytosolic Ca^{2+} (<1 μM). Proteoliposomes containing purified rabbit skeletal muscle Ca^{2+} release channels were fused with planar lipid bilayer membranes, and single-channel activities were recorded in symmetric 0.25 M KCl media. The SR lumenal to cytosolic Ca^{2+} fluxes were varied by changing lumenal Ca^{2+} concentrations, holding potentials, and by adding different concentrations of other competing ions. Our results indicated that lumenal Ca^{2+} flowing through the channel can both activate and inhibit the skeletal muscle Ca^{2+} release channel. A preliminary report of this work has been presented in abstract form (Tripathy and Meissner, 1995)

MATERIALS AND METHODS

Materials

Phospholipids were obtained from Avanti Polar Lipids (Birmingham, AL). All other chemicals were of analytical grade.

Preparation of heavy SR vesicles and purification and reconstitution of Ca^{2+} release channel

"Heavy" SR vesicle fractions enriched in [^{3}H]ryanodine binding and Ca^{2+} release channel activities were prepared from rabbit skeletal muscle in the presence of protease inhibitors (100 nM aprotinin, 1 μM leupeptin, 1 μM pepstatin, 1 mM benzamidine, 0.2 mM phenylmethylsulfonyl fluoride) as described (Meissner, 1984). The 3-[(3-cholamidopropyl)dimethylammonio]-1-propanesulfonate (CHAPS)-solubilized skeletal muscle 30 S Ca^{2+} release channel complex was purified and reconstituted into proteoliposomes by removal of CHAPS by dialysis (Lee et al., 1994). Proteoliposomes were sedimented by centrifugation, resuspended in 0.3 M sucrose, 5 mM KPIPES (potassium piperazine-*N,N'*-bis(2-ethanesulfonic acid), pH 7.4, quick frozen and stored at −80°C. After prolonged storage, the proteoliposomes tended to aggregate. A brief sonication of 15–20 s was sufficient to break up the aggregates.

Single-channel measurements

Unless otherwise stated, single-channel recordings were performed in symmetric KCl buffer solution (0.25 M KCl, 10 mM KPIPES, pH 7.1) containing the additions indicated in the text. Proteoliposomes containing the purified skeletal muscle Ca^{2+} release channel were added to the *cis* chamber of a bilayer apparatus and fused in the presence of an osmotic gradient (250 mM *cis* KCl/50 mM *trans* KCl) with Mueller-Rudin–type planar bilayers containing a 4:1 mixture of bovine brain phosphatidylethanolamine and phosphatidylcholine (30–40 mg of total phospholipid/ml of *n*-decane). After the appearance of single-channel activity, further fusion of proteoliposomes was prevented by increasing *trans* [KCl] to 0.25 M. The *trans* side of the bilayer was defined as ground. The sidedness of channel orientation was determined by testing the sensitivity of the channel to cytosolic Ca^{2+} and ATP. Proteoliposomes fused with the bilayers in such a way that in a majority of recordings (>98%) the cytosolic side of the Ca^{2+} release channel faced the *cis* side and the lumenal side the *trans* side of the bilayer. Data from the small number of channels (2%) that incorporated in the reverse direction were not used in this study. Channel activities were recorded using a commercially available patch-clamp amplifier with a bilayer headstage (Axopatch 1D; Axon Instruments, Burlingame, CA). Recordings were filtered at 4 kHz through an eight-pole, low-pass Bessel filter (Frequency Devices) and digitized at 20 kHz. Data acquisition and analysis were performed with the software package pClamp 6.0.1. (Axon Instruments) using an IBM-compatible computer and a 12-bit A/D–D/A converter (Digidata 1200; Axon Instruments). Data files were directly acquired into the hard disk of the computer using the Clampex pulse protocol (100–200 episodes of 358 ms) or by continuous Fetchex mode (file length 120 s).

Single-channel data analysis

Most commonly, the threshold (ϕ) for an event detection is set at 50% of the difference between the levels. The advantage of this threshold setting is that the event durations are not biased, because the values for the threshold are the same for both opening and closing transitions (Sachs et al., 1982). However, short events with open durations on the order of the filter rise time (T_r) are greatly underestimated, and events shorter than about $T_r/2$ are missed altogether, because after filtering they never reach the threshold. Our single-channel recordings were filtered during analysis by a digital gaussian filter at 2 kHz. This gave an effective cutoff frequency of 1.8 kHz, taking into account the cutoff frequency of 4 kHz during data acquisition. Thus, the T_r was approximately 167 μs (*The Axon Guide for Electrophysiology and Biophysics Laboratory Techniques*, Axon Instruments, Inc., 1993, p. 138.). We observed that millimolar levels of ATP caused very short closed to open transitions (see Results) and found that the number of events was greatly underestimated by a 50% threshold analysis. To increase the probability of short events being scored, the threshold was kept at 25% of channel amplitude. The rms noise (σ) in our recordings was about 0.6 pA. Therefore, the ϕ/σ ratio was always greater than 5, which ensured that no noise peaks were counted (Colquhoun and Sigworth (1983) recommend that the ϕ/σ ratio be greater than 3–5). The 25% threshold analysis slightly overestimated the open time constants. An empirical comparison of open time constants obtained from the same data at 25% and 50% threshold analysis showed that the overestimation was <5% for the short and <15% for the long open time constant. The closed time constants were not calculated.

Calculation of ionic flux

All of our experiments were done in mixed ionic solutions that contained K^+ and Ca^{2+}, and where indicated Ba^{2+} or Mg^{2+}. To calculate the individual ionic fluxes, we used a model describing the ionic conduction of the sheep cardiac Ca^{2+} release channel (Tinker et al., 1992, 1993). The model is based on Eyring rate theory and assumes single ion occupancy and a symmetrical, voltage- and concentration-independent energy profile with four barriers and three binding sites. The model predicts the conduction properties of the purified and native cardiac channel with both monovalent and divalent cations as permeant species. To determine whether the model can predict the conduction properties of the skeletal release channel, we compared single-channel current-voltage (*I-V*) curves obtained from our experiments in symmetrical 0.25 M KCl with a lumenal [Ca^{2+}] of 5 or 10 mM and nominally zero cytosolic Ca^{2+} with those obtained from the model under the same ionic conditions. There was excellent fit between our *I-V* curves and those calculated from the model, which gave us the confidence to use this model to calculate individual ionic fluxes from experiments done in mixed ionic conditions. We have used the energy profile values for K^+, Ca^{2+}, Mg^{2+}, and Ba^{2+} as given in tables I and II in Tinker et al. (1992, 1993).

Determination of free Ca^{2+} concentrations

Different free Ca^{2+} concentrations were obtained by mixing appropriate amounts of $CaCl_2$ and EGTA as determined using the stability constants and computer program published by Shoenmakers et al. (1992). In some cases free Ca^{2+} concentrations were measured using a Ca^{2+}-selective electrode (World Precision Instruments, Sarasota, FL).

Data analysis

Results are given as means ± SE, with the number of experiments in parentheses. Significance of differences of data was analyzed with Stu-

dent's paired t-test. Differences were regarded to be statistically significant at $p < 0.05$.

RESULTS

Ca^{2+} release channel activity with cytosolic Ca^{2+} as the activating ligand

The skeletal muscle Ca^{2+} release channel conducts Ca^{2+} and exhibits a Ca^{2+}-sensitive channel activity (Meissner, 1994). It was therefore conceivable that Ca^{2+} flowing through the channel regulates Ca^{2+} release channel activity by positive and negative feedback mechanisms. To distinguish between the effects of SR lumenal and cytosolic Ca^{2+} on channel activity, single purified Ca^{2+} release channels were inserted into planar lipid bilayers and recorded in symmetric 0.25 M KCl media with varying Ca^{2+} concentrations in the *trans* (SR lumenal) and *cis* (cytosolic) chambers of the bilayer apparatus. The skeletal Ca^{2+} release channel has been shown to conduct monovalent ions more efficiently than Ca^{2+} and to be impermeant to Cl^-. Therefore, the measured currents were mostly carried by K^+ and not Ca^{2+}. With K^+ as the current carrier, single-channel conductance was ~770 pS (Xu et al., 1993).

In preliminary experiments, we determined the voltage dependence of the skeletal muscle Ca^{2+} release channel, with Ca^{2+} as the solely activating ligand. Channels were recorded in symmetric 0.25 M KCl media containing a low (<0.05 μM) or optimally activating concentration of 50 μM free Ca^{2+} (Meissner, 1994). In the presence of <0.05 μM free Ca^{2+} on both sides of the bilayer, the release channels exhibited very infrequent and brief openings at holding potentials of −40 mV and +40 mV (Fig. 1, *upper two recordings*). The number of channel openings was greatly increased at both holding potentials when the cytosolic and lumenal [Ca^{2+}] were maintained at 50 μM (*middle two recordings*). The subsequent decrease in lumenal [Ca^{2+}] to <0.05 μM did not markedly change the gating behavior of the channel (Fig. 1, *bottom recordings*). With 50 μM free Ca^{2+} in both bilayer chambers, the channel displayed a small but significantly higher channel open probability (P_o) at holding potentials of +40 mV and +60 mV than at holding potentials of −40 mV or −60 mV. The mean P_os at +40 and −40 mV holding potentials were 0.19 ± 0.02 and 0.14 ± 0.02, respectively ($n = 28$, $p < 0.01$) (Table 1). The mean P_os at +60 and −60 mV holding potentials were 0.25 ± 0.05 and 0.12 ± 0.03, respectively ($n = 12$, $p < 0.01$). Analysis of the dwell times showed that both the open and closed times of cytosolic Ca^{2+}-activated channels could be fitted by the sum of two exponentials (data not shown). The short and long open time constants were significantly higher at +40 mV and +60 mV than at −40 mV and −60 mV, but all had a mean duration of less than 1 ms (Table 1). A decrease in lumenal [Ca^{2+}] from 50 μM to <0.05 μM did not cause any significant change in the channel parameters of Table 1. As in the case of symmetrical 50 μM Ca^{2+}, the channel displayed a small but

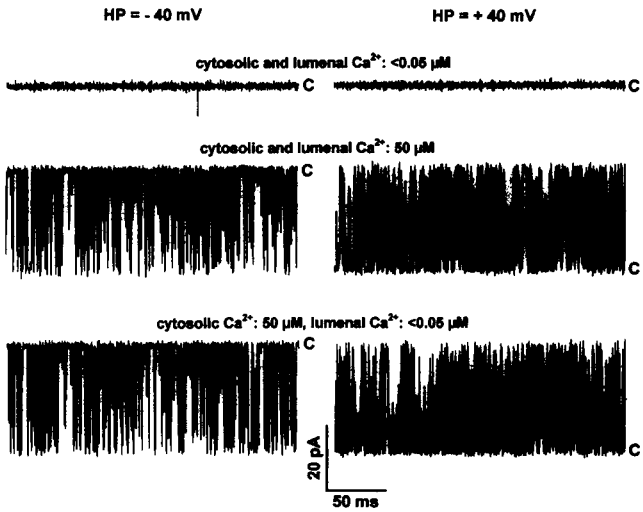

FIGURE 1 Effect of cytosolic and lumenal [Ca^{2+}] and holding potential on Ca^{2+} release channel activity. (*A*) Shown are six recordings, the upper two from one experiment and the lower four from a different experiment. Single channel currents, shown as downward or upward deflections from closed levels (marked C), were recorded in symmetrical 0.25 M KCl, 10 mM KPIPES, pH 7.1. Current recordings were obtained at −40 mV (*left*) and +40 mV (*right*) holding potential. The *cis* and *trans* chamber solutions also contained: (*Top recordings*) 2 mM EGTA and 150 μM $CaCl_2$ (45 nM free Ca^{2+}, both cytosolic and lumenal). Both left and right panels, $P_o <$ 0.0001. (*Middle recordings*) 100 μM EGTA and 150 μM $CaCl_2$ (50 μM free Ca^{2+}, both cytosolic and lumenal). Left panel, $P_o = 0.17$; right panel, $P_o = 0.18$. (*Bottom recordings*) cytosolic: 100 μM EGTA and 150 μM $CaCl_2$ (50 μM free Ca^{2+}); lumenal: 2 mM EGTA and 150 μM $CaCl_2$ (45 nM free Ca^{2+}). Left panel, $P_o = 0.17$; right panel, $P_o = 0.22$.

significantly higher P_o at +40 mV than at −40 mV holding potential. Thus, the Ca^{2+} release channel showed only a weak voltage dependence when recorded with 50 μM cytosolic Ca^{2+} as the activating ligand. Channel activities were somewhat higher at positive than negative holding potentials and were characterized by short (<1 ms) open events.

We also determined the effects of cytosolic Ca^{2+} on channel activity in the presence of ATP, an activator of the skeletal muscle Ca^{2+} release channel (Meissner, 1994), because a majority of our single-channel measurements were done in the presence of 2 mM cytosolic ATP. In the upper two traces of Fig. 2 *A*, the free cytosolic and lumenal [Ca^{2+}] were kept at 45 nM and a single channel was recorded in the presence of 2 mM cytosolic ATP at +40 mV and −40 mV. Comparison with the upper two recordings in Fig. 1 *A* shows that the addition of 2 mM ATP greatly increased the frequency of short channel openings at both holding potentials. Channel activity dramatically increased when the free cytosolic [Ca^{2+}] was raised from 45 nM to 0.5 μM (Fig. 2 *A*, *second traces*), 2.5 μM (*third traces*), and 10 μM (*bottom traces*). In the presence of 10 μM cytosolic Ca^{2+} and 2 mM cytosolic ATP, nearly maximally activated channel activities were obtained ($P_o = 0.9$; Fig. 2 *B*). There were no significant differences in activity between +40 mV

TABLE 1 Effect of lumenal Ca^{2+} on channel parameters

		Cytosolic Ca^{2+} (μM)						
		<0.1	50	50	<0.1 (+2 mM ATP)			
		Lumenal Ca^{2+} (μM)						
HP (mV)	Channel parameters	<0.1	<0.1	50	<0.1	50	250	5000
−40	No. of events	22 ± 21	61,907 ± 13,707	56,412 ± 7,478	21,385 ± 13,169	16,112 ± 2,586	21,197 ± 8,760	29,635 ± 11,175
	P_o	<0.0001	0.16 ± 0.02	0.14 ± 0.02	0.01 ± 0.00	0.22 ± 0.05*	0.27 ± 0.09*	0.19 ± 0.07*
	A_{o1}	—	0.77 ± 0.02	0.79 ± 0.03	0.96 ± 0.03	0.40 ± 0.06*	0.47 ± 0.14*	0.60 ± 0.08*
	A_{o2}	—	0.23 ± 0.02	0.21 ± 0.03	0.04 ± 0.03	0.60 ± 0.06*	0.53 ± 0.14*	0.40 ± 0.08*
	τ_{o1} (ms)	—	0.14 ± 0.02	0.14 ± 0.01	0.08 ± 0.01	0.74 ± 0.17*	1.49 ± 0.27*	0.62 ± 0.09*
	τ_{o2} (ms)	—	0.46 ± 0.03	0.43 ± 0.02	0.28 ± 0.04	3.05 ± 0.72*	6.51 ± 2.12*	1.99 ± 0.37*
+40	No. of events	7 ± 5	69,403 ± 8,810	71,273 ± 6,818	16,716 ± 6,424	20,006 ± 2,815	27,088 ± 12,938	28,034 ± 8,332
	P_o	<0.0001	0.20 ± 0.02**	0.19 ± 0.02**	0.01 ± 0.00	0.03 ± 0.01	0.03 ± 0.02	0.14 ± 0.06*
	A_{o1}	—	0.71 ± 0.04	0.70 ± 0.04**	0.97 ± 0.02	1.00 ± 0.00	0.89 ± 0.09	0.58 ± 0.10*
	A_{o2}	—	0.29 ± 0.04	0.30 ± 0.04**	0.03 ± 0.02	0.00 ± 0.00	0.11 ± 0.09	0.42 ± 0.10*
	τ_{o1} (ms)	—	0.14 ± 0.02	0.17 ± 0.01**	0.09 ± 0.00	0.16 ± 0.01	0.15 ± 0.02	0.43 ± 0.21*
	τ_{o2} (ms)	—	0.53 ± 0.03**	0.54 ± 0.04**	0.29 ± 0.05	—	0.62 ± 0.26	2.02 ± 0.86*

Channel parameters were obtained from 2-min continuous recordings as described in Materials and Methods. P_o refers to channel open probability and was calculated from single-channel and multiple-channel recordings. Open-time data were obtained from single-channel recordings and fitted by the maximum likelihood method to the probability density function: $f(t) = \Sigma A_i(1/\tau_i) \exp(-t/\tau_i)$, where A_i and τ_i are the relative areas of the distributions and time constants of the *ith* state, respectively (Colquhoun and Sigworth, 1983). Values are mean ± SE of 4–28 experiments, except those in column 3, which are given as mean ± SD of three experiments.

**Significant difference between values at holding potentials of +40 mV and −40 mV ($p < 0.05$; $n = 3$–28).

*Significant difference between values at <0.1 μM lumenal [Ca^{2+}] and the indicated lumenal [Ca^{2+}] ($p < 0.05$; $n = 4$–11).

and −40 mV when the free cytosolic [Ca^{2+}] was varied from 45 nM to 10 μM (Fig. 2 *B*). As observed earlier (Smith et al., 1986), the mean open time constants increased as the cytosolic [Ca^{2+}] was increased. The two mean open time constants at −40 mV increased from 0.08 ± 0.01 ms and 0.28 ± 0.04 ms at 45 nM cytosolic Ca^{2+} to 1.26 ± 0.04 ms and 28.7 ± 10.3 ms ($n = 3$). Essentially identical increases in open time constants were seen at +40 mV. The data of Fig. 2 suggested that the addition of ATP to the cytosolic side did not introduce voltage sensitivity to channel activity. Furthermore, the data confirmed that the combined presence of cytosolic Ca^{2+} and ATP results in the appearance of open events with time constants of several milliseconds and in an almost optimal activation of channels.

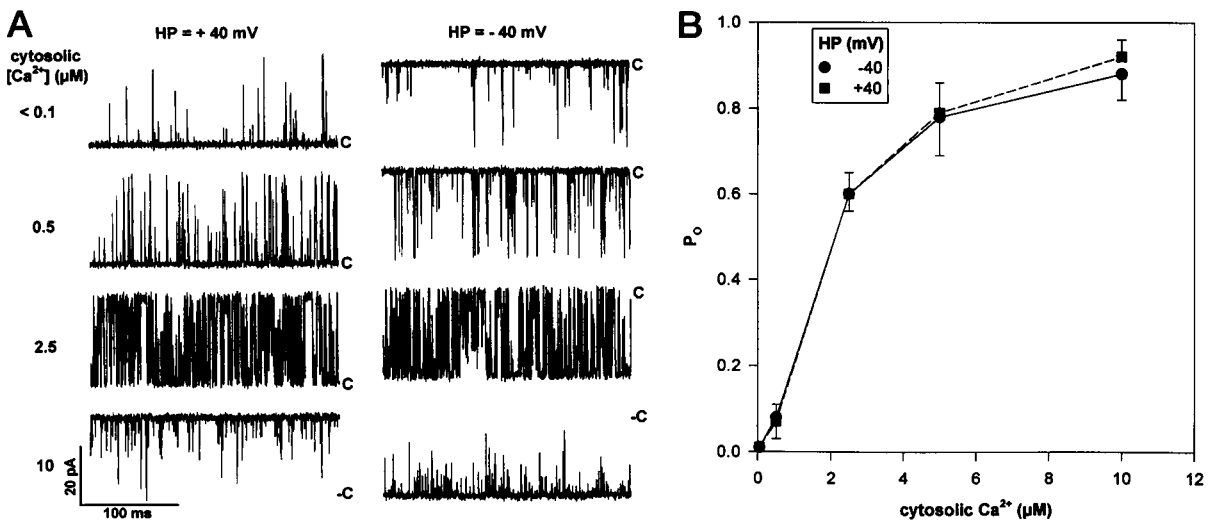

FIGURE 2 Effect of varying cytosolic Ca^{2+} on P_o and gating of cytosolic ATP-activated channel at nM lumenal Ca^{2+}. (*A*) Shown are eight recordings from one experiment. Single-channel currents, shown as downward or upward deflections from closed levels (marked C), were recorded in symmetrical 0.25 M KCl, 10 mM KPIPES, pH 7.1. The *trans* chamber solution also contained 2 mM EGTA and 150 μM $CaCl_2$ (45 nM free Ca^{2+}), and the *cis* chamber solution the indicated free [Ca^{2+}]. Current recordings were obtained at +40 mV (*left*) and −40 mV (*right*) holding potential. (*Top recordings*) Left panel, $P_o = 0.009$, right panel, $P_o = 0.008$. (*Second recordings*) Left panel, $P_o = 0.035$; right panel, $P_o = 0.024$. (*Third recordings*) Left panel, $P_o = 0.60$; right panel, $P_o = 0.60$. (*Bottom recordings*) Left panel, $P_o = 0.98$; right panel, $P_o = 0.98$. (*B*) Mean P_o values were plotted against free cytosolic [Ca^{2+}]. P_o values were obtained from recordings as in *A* at holding potentials of −40 and +40 mV. Data points are means ± SE of five experiments.

Regulation of cytosolic ATP-activated Ca^{2+} release channel by 50 μM lumenal Ca^{2+} and membrane potential

Single ATP-activated channels displayed a profound voltage dependence when recorded at an elevated lumenal [Ca^{2+}] but low cytosolic [Ca^{2+}]. In Fig. 3 (*top two traces*) a single channel was recorded at 50 μM lumenal [Ca^{2+}] in the presence of a low cytosolic Ca^{2+} concentration (45 nM free Ca^{2+}) and 2 mM cytosolic ATP. Channel activity was substantially higher at −40 mV than at +40 mV, and the durations of the open events were longer at −40 mV than at +40 mV (for a quantitative description of P_o and open time constants, see below and Table 1). Reduction of lumenal [Ca^{2+}] to <1 μM decreased P_o and led to the disappearance of the long open events at −40 mV without noticeably affecting single-channel activity at +40 mV (Fig. 3, *middle recordings*). A subsequent increase of lumenal [Ca^{2+}] showed that the effects of 50 μM lumenal Ca^{2+} were fully reversible (Fig. 3, *bottom recordings*).

A negative holding potential favors cation movements from the *trans* (SR lumenal) side to the *cis* (cytosolic) side of the bilayer. Our observation of a lumenal Ca^{2+}-dependent increase in P_o at a negative but not positive holding potential (Fig. 3) therefore suggested to us that Ca^{2+} ions flowing through the open channel may activate the channel by binding to cytosolically located Ca^{2+} sites. We further tested the idea of a regulation of Ca^{2+} release channel activity by lumenal Ca^{2+} by recording the effects of varying lumenal to cytosolic Ca^{2+} fluxes on channel activation and gating. Channels were recorded in the presence of 2 mM cytosolic ATP because ATP greatly augmented the activating effects of cytosolic Ca^{2+} (Fig. 2). Different lumenal to cytosolic Ca^{2+} fluxes were obtained by varying lumenal [Ca^{2+}] and holding potentials. In other experiments, Ca^{2+} fluxes were decreased by adding other divalent cations (Mg^{2+}, Ba^{2+}) to the lumenal chamber or by increasing [KCl]. In each case, an attempt was made to correlate Ca^{2+} fluxes with channel activities by calculating channel-mediated Ca^{2+} fluxes using the model of Tinker et al. (1992, 1993) (see Materials and Methods).

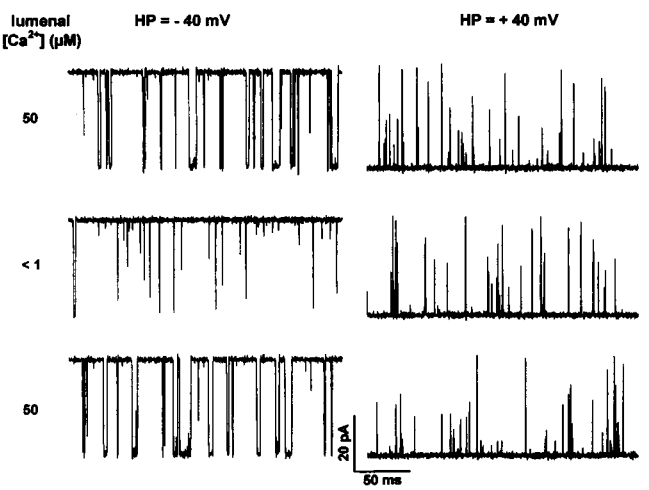

FIGURE 3 Effect of 50 μM lumenal Ca^{2+} on P_o and gating of cytosolic ATP-activated channel at nanomolar cytosolic Ca^{2+}. Shown are six recordings from a single experiment. The recordings in the left panel were obtained at −40 mV holding potential, and the recordings in the right panel at +40 mV holding potential. Single-channel currents, shown as upward (*right panels*) or downward (*left panels*) deflections from the closed levels, were recorded in symmetrical 250 mM KCl, 10 mM KPIPES, pH 7.1 media. The *cis* chamber solution contained 2 mM ATP, 150 μM $CaCl_2$, and 2 mM EGTA (45 nM free Ca^{2+}). The *trans* chamber solution contained the following: (*Top recordings*) 150 μM $CaCl_2$ and 100 μM EGTA (50 μM free Ca^{2+}). Left panel, P_o = 0.13; right panel, P_o = 0.015. (*Middle recordings*) 150 μM $CaCl_2$ and 200 μM EGTA (0.66 μM free Ca^{2+}). Left panel, P_o = 0.006; right panel, P_o = 0.015. (*Bottom recordings*) 200 μM EGTA and 250 μM $CaCl_2$ (50 μM free Ca^{2+}). Left panel, P_o = 0.13; right panel, P_o = 0.01.

Effects of <1 μM to 10 mM lumenal Ca^{2+} and membrane potential on cytosolic ATP-activated Ca^{2+} release channel

Lumenal [Ca^{2+}] was varied from <1 μM to 10 mM, and channel activities were recorded at a low cytosolic [Ca^{2+}] at holding potentials ranging from −60 mV to +60 mV. Fig. 4 shows a typical channel recording in which a single release channel was monitored in the presence of 2 mM ATP and 45 nM cytosolic Ca^{2+} at holding potentials of −40 mV (*A*), +20 mV (*B*), and +40 mV (*C*). In the three panels, lumenal [Ca^{2+}] was increased stepwise from 0.66 μM to 50 μM, 250 μM, 1 mM, 5 mM, and 10 mM (from top to bottom). Inspection of the single-channel recordings at −40 mV shows that the duration of the open events increased from <1 ms to several milliseconds as lumenal [Ca^{2+}] was increased from 0.66 μM to 50 μM and 250 μM, and then again decreased as lumenal [Ca^{2+}] was further increased to 1, 5, and 10 mM. Fig. 4 *A* also shows a significant reduction in single-channel conductances by millimolar levels of lumenal [Ca^{2+}], which suggested, in agreement with previous reports (Tinker et al., 1992; Xu et al., 1993), blockade of K^+ currents by Ca^{2+}. At +20 mV (Fig. 4 *B*) and +40 mV (Fig. 4 *C*), similar increases in P_o and the duration of open events were recorded as the lumenal [Ca^{2+}] was increased, except that higher lumenal [Ca^{2+}] was required to observe an increase in P_o and the appearance of open events with a duration longer than 1 ms. At +20 mV, increased P_o and long-duration open events first appeared as lumenal [Ca^{2+}] was raised to 1 mM (and peaked at a lumenal [Ca^{2+}] of 5 mM), whereas at +40 mV a lumenal [Ca^{2+}] of 5–10 mM was required to observe a substantial increase in P_o and the duration of open events. At +60 mV, P_o and the duration of open events did not appreciably increase at lumenal [Ca^{2+}] as high as 10 mM (data not shown).

In Fig. 5, *A* and *B*, the mean P_o values of several cytosolic ATP-activated channels (n = 6–11) are plotted against lumenal pCa at six different holding potentials (Fig. 5 *A*) and against holding potential at six different lumenal [Ca^{2+}] (Fig. 5 *B*). Data of Fig. 5, *A* and *B*, confirmed that channel activity depended on both lumenal [Ca^{2+}] and holding

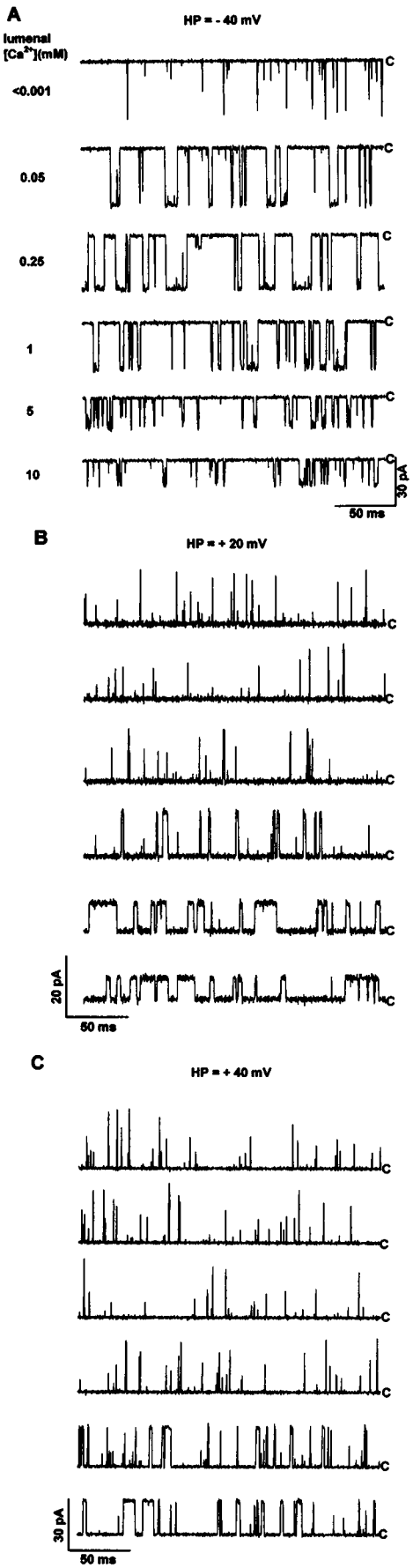

potential, but also showed that neither parameter by itself determined channel activity in a straightforward manner. By comparison, a good correlation was obtained when we considered both values together by calculating the lumenal to cytosolic Ca^{2+} fluxes at the various lumenal [Ca^{2+}] and holding potentials according to the model of Tinker et al. (1992, 1993). In Fig. 5 *C*, P_o is plotted against these values. Most of the points could be reasonably well fitted by a single curve, with the exception of two points at +20 mV holding potential (corresponding to a lumenal [Ca^{2+}] of 5 and 10 mM). The reason for the two outlying P_o values is unclear. Fig. 5 *C* shows that a Ca^{2+} flux of up to ~1.25 pA led to channel activation, whereas higher Ca^{2+} fluxes appeared to inhibit channel activity.

The effects of lumenal [Ca^{2+}] and holding potential on channel activity were analyzed by carrying out a detailed time analysis of ATP-activated channels recorded at lumenal [Ca^{2+}] of 45 nM to 10 mM. The open time histograms could be best fitted by the sum of two exponentials (not shown). Table 1 lists the number of events, P_o values, and open channel parameters obtained at lumenal [Ca^{2+}] of 45 nM, 50 μM, 250 μM, and 5 mM. The data show that the increases in channel activity at −40 mV holding potential and at lumenal [Ca^{2+}] of 50 and 250 μM (Fig. 4 *A*) could be largely accounted for by an increase in the mean durations of the short and open long events. Decreased channel activities observed at millimolar levels of lumenal [Ca^{2+}] and −40 mV could also be accounted for by a shortening of the mean durations of the open events. As shown in Fig. 4, *B* and *C*, at +20 mV and +40 mV, long open events first appeared as lumenal [Ca^{2+}] was raised to 1 and 5 mM, respectively. The increase in open time constants (τ_{01} = 0.43 ± 0.21 ms, τ_{02} = 2.02 ± 0.86 ms) led to an increased P_o at a lumenal [Ca^{2+}] of 5 mM and holding potential of +40 mV (Table 1). The two corresponding time constants at 1 mM and 10 mM lumenal Ca^{2+} were 0.25 ± 0.06 ms and 1.47 ± 0.37 ms, and 1.10 ± 0.37 ms and 3.96 ± 1.39 ms (n = 5), respectively. At +20 mV, the two open time constants

FIGURE 4 Effect of increasing lumenal [Ca^{2+}] from <1 μM to 10 mM on activity and gating of ATP-activated channel at nanomolar cytosolic Ca^{2+} and different holding potentials. All recordings are from a single experiment. Holding potentials were −40 mV (*A*), +20 mV (*B*), and +40 mV (*C*). Single-channel currents, shown as upward or downward deflections from the closed levels (marked C), were recorded in symmetrical 250 mM KCl, 10 mM KPIPES, pH 7.1 media. The *cis* chamber solution contained 2 mM ATP, 150 μM $CaCl_2$, and 2 mM EGTA (45 nM free Ca^{2+}). The *trans* chamber solution contained the following: (*Top recordings*) 150 μM $CaCl_2$ and 200 μM EGTA (0.66 μM free Ca^{2+}). The P_o values were: (*A*) P_o = 0.006; (*B*) P_o = 0.009; (*C*) P_o = 0.008. (*Second recordings*) 250 μM $CaCl_2$ and 200 μM EGTA (50 μM free Ca^{2+}). (*A*) P_o = 0.13; (*B*) P_o = 0.006; (*C*) P_o = 0.008. (*Third recordings*) 450 μM $CaCl_2$ and 200 μM EGTA (250 μM free Ca^{2+}). (*A*) P_o = 0.28; (*B*) P_o = 0.006; (*C*) P_o = 0.003. (*Fourth recordings*) 1.2 mM $CaCl_2$ and 200 μM EGTA (1 mM free Ca^{2+}). (*A*) P_o = 0.13; (*B*) P_o = 0.03; (*C*) P_o = 0.008. (*Fifth recordings*) 5.2 mM $CaCl_2$ and 200 μM EGTA (5 mM free Ca^{2+}). (*A*) P_o = 0.06; (*B*) P_o = 0.37; (*C*) P_o = 0.07. (*Bottom recordings*) 10.2 mM $CaCl_2$ and 200 μM EGTA (10 mM free Ca^{2+}). (*A*) P_o = 0.06; (*B*) P_o = 0.26; (*C*) P_o = 0.09.

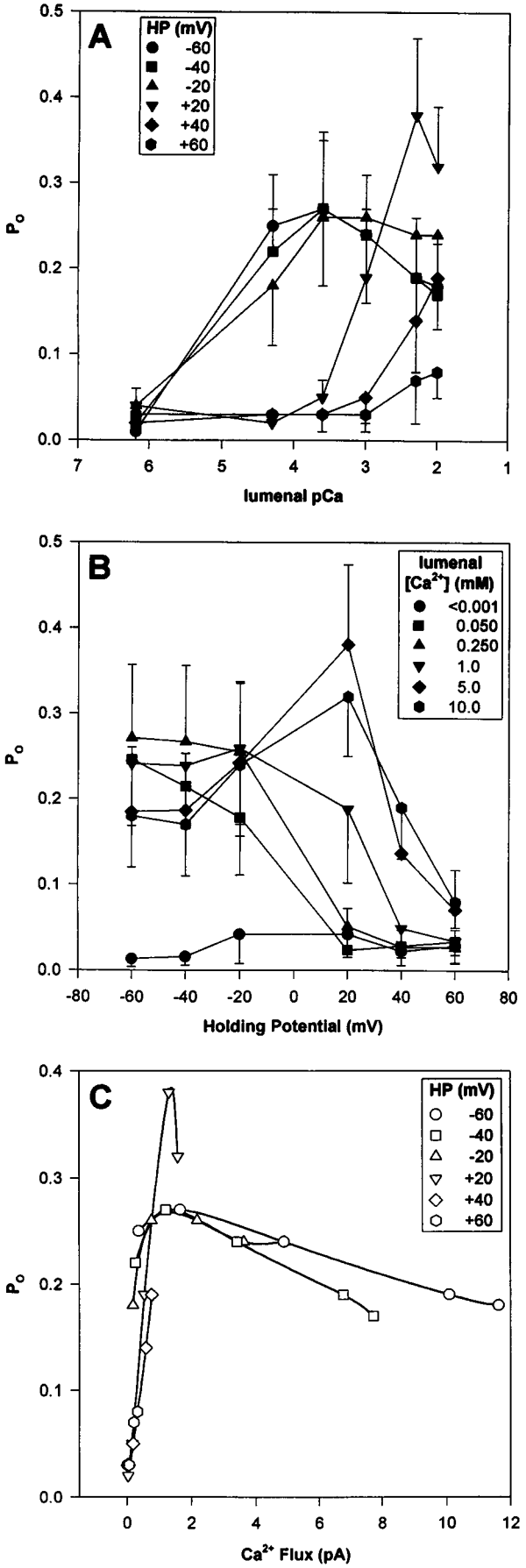

increased from 0.13 ± 0.02 ms and 0.52 ± 0.12 ms at 50 μM lumenal Ca^{2+} to 0.94 ± 0.52 ms and 3.72 ± 2.26 ms at 1 mM lumenal Ca^{2+}, 1.69 ± 0.29 ms and 9.08 ± 2.56 ms at 5 mM lumenal Ca^{2+}, and 1.73 ± 0.41 ms and 5.80 ± 1.04 ms at 10 mM lumenal Ca^{2+} (n = 5). At 45 nM and 50 μM lumenal Ca^{2+}, the number of resolvable events was 3–4 times lower for ATP-activated channels than for 50 μM cytosolic Ca^{2+}-activated channels (Table 1). The number of events increased as the lumenal [Ca^{2+}] was raised from 50 μM to 5 mM, but stayed well below the number of events observed for the cytosolic Ca^{2+}-activated channels. Taken together with the data of Figs. 4 and 5, our results indicated that for ATP-activated channels, there existed a good correlation between channel open probabilities, open time constants, and lumenal to cytosolic Ca^{2+} fluxes.

Sitsapesan and Williams (1995) recently reported that 1 mM cytosolic ATP did not activate the sheep skeletal muscle Ca^{2+} release channel when cytosolic and lumenal [Ca^{2+}] was reduced to picomolar levels. We observed that rabbit skeletal muscle Ca^{2+} release channels were activated by 2 mM cytosolic ATP when both the cytosolic and lumenal [Ca^{2+}] was reduced to nominal levels (60 pM) (four of four experiments; data not shown). Single-channel activities and the number of channel events did not decrease as lumenal [Ca^{2+}] was reduced from ~1 μM to 60 pM. These experiments were carried out at pH 7.4 to achieve picomolar levels of free Ca^{2+}. In two (of two) experiments we observed an activation of Ca^{2+} release channels by 2 mM cytosolic ATP at picomolar cytosolic and lumenal Ca^{2+} when SR vesicles were fused with the bilayers (data not shown). This result suggested that it is unlikely that the differences in channel opening observed by Sitsapesan and Williams (1995) and us in the presence of cytosolic ATP at pM lumenal and cytosolic Ca^{2+} were due to the use of native and purified channels, respectively.

Effect of 50 μM lumenal [Ca^{2+}] on channel activity at submicromolar cytosolic Ca^{2+}

Ca^{2+} release channels responded to a lumenal [Ca^{2+}] of 50 μM and membrane potential in the absence of ATP when

FIGURE 5 Dependence of ATP-activated channel activities and channel-mediated Ca^{2+} fluxes on lumenal Ca^{2+} concentration and holding potential. Channel recordings were made in symmetrical 250 mM KCl, 10 mM KPIPES, pH 7.1. The *cis* chamber solution contained 2 mM ATP, 150 μM $CaCl_2$, and 2 mM EGTA (45 nM free Ca^{2+}). *Trans* chamber solution initially contained 0.66 μM free Ca^{2+} (150 μM $CaCl_2$ and 200 μM EGTA). Lumenal free [Ca^{2+}] was stepwise increased to 0.05, 0.25, 1, 5, and 10 mM. At each lumenal [Ca^{2+}], ±20, ±40 and ±60 mV holding potentials were applied and the channel activity was recorded. (*A*) P_o as a function of lumenal pCa at the indicated holding potentials. Data are the mean ± SE of 6–11 experiments. (*B*) P_o as a function of holding potential at the indicated free lumenal [Ca^{2+}]. Data are the mean ± SE of 6–11 experiments. (*C*) P_o as a function of lumenal to cytosolic Ca^{2+} fluxes. Ca^{2+} fluxes at various lumenal [Ca^{2+}] and holding potentials were calculated using the model of Tinker et al. (1992, 1993). Lumenal [Ca^{2+}] at each of the indicated holding potentials was 50 μM, 250 μM, 1 mM, 5 mM, and 10 mM (from left to right). Ca^{2+} fluxes of ≥10 pA significantly inhibited channel activity.

channels were activated by suboptimal cytosolic [Ca^{2+}]. The top two recordings in Fig. 6 show the current recordings of a single channel at holding potentials of −40 mV (*left*) and +40 mV (*right*) with 50 μM lumenal Ca^{2+} and 0.44 μM cytosolic Ca^{2+}. In the two bottom recordings lumenal Ca^{2+} was reduced to <1 μM by the addition of EGTA. Although the level of channel activation was small under these recording conditions, differences in channel activity could be observed. Ca^{2+} channel activity at 50 μM lumenal Ca^{2+} was significantly higher at −40 mV (P_o = 0.010 ± 0.003, n = 4) than at +40 mV (P_o = 0.005 ± 0.002, n = 4). It should be noted that this voltage dependence was opposite that observed for channels recorded in a symmetric 50 μM Ca^{2+} solution (Fig. 1 *A*) but similar to that for lumenal Ca^{2+}- and cytosolic ATP-activated channels (Figs. 3 and 4 *A*). Furthermore, as observed for ATP-activated channels, a decrease in lumenal [Ca^{2+}] from 50 μM to <1 μM lowered P_o at −40 mV (from 0.010 ± 0.003 to 0.004 ± 0.001) but not at +40 mV (0.005 ± 0.002 and 0.004 ± 0.001). The open time data could be fitted by one exponential in these experiments (not shown). An increase in the number of channel events (1.4-fold, not significant) and the open time constant (1.7-fold, significant) led to the increased P_o observed at −40 mV in the presence of 50 μM lumenal Ca^{2+}. Thus, 50 μM lumenal Ca^{2+} increased channel activity at −40 mV by significantly increasing the open time constant compared to the value at +40 mV.

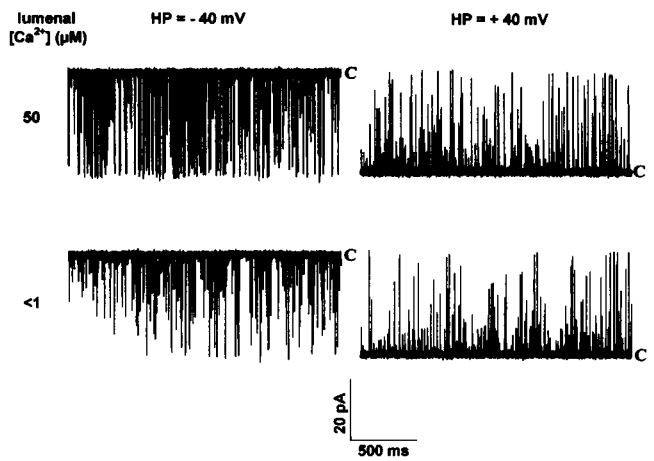

FIGURE 6 Effect of 50 μM lumenal Ca^{2+} on Ca^{2+} release channel activity at suboptimal cytosolic Ca^{2+}. All recordings are from a single experiment. Single-channel currents, shown as downward or upward deflections from the closed levels (marked C), were recorded in symmetrical 0.25 M KCl, 10 mM KPIPES, pH 7.1. The left panel recordings were obtained at −40 mV and the right panel recordings at +40 mV holding potential. The *cis* chamber solution also contained 500 μM EGTA and 250 μM $CaCl_2$ (0.44 μM free Ca^{2+}). The *trans* chamber solutions contained: (*Top recordings*) 100 μM EGTA and 150 μM $CaCl_2$ (50 μM free Ca^{2+}). Left panel, P_o = 0.010 ± 0.003, no. of events = 5028 ± 1326, τ_o = 0.290 ± 0.04. Right panel, P_o = 0.005 ± 0.002, no. of events = 3607 ± 1148, τ_o = 0.167 ± 0.01. (*Bottom recordings*) 200 μM EGTA and 150 μM $CaCl_2$ (0.66 μM free Ca^{2+}). Left panel, P_o = 0.004 ± 0.001, no. of events = 3234 ± 658, τ_o = 0.177 ± 0.01. Right panel, P_o = 0.004 ± 0.001, no. of events = 3490 ± 859, τ_o = 0.162 ± 0.02. Values are mean ± SE of four experiments. Channel parameters were obtained from 2-min continuous recordings as described in Materials and Methods.

Effects of [KCl], lumenal Mg^{2+}, and lumenal Ba^{2+} on channel activity

We further tested the idea that SR lumenal to cytosolic Ca^{2+} fluxes activate the release channel by reducing channel-mediated Ca^{2+} fluxes while maintaining a [Ca^{2+}] of 50 μM in the *trans* bilayer chamber. The *cis* chamber contained 45 nM cytosolic Ca^{2+} and 2 mM cytosolic ATP. In one set of experiments, we reduced the Ca^{2+} fluxes by increasing the [KCl] in the recording solutions. Channel-mediated Ca^{2+} fluxes were reduced by increasing the [KCl] in both chambers from 0.25 M to 1 M. In Fig. 7 *A* (*upper two recordings*), two cytosolic ATP-activated release channels were initially recorded in a symmetric 0.25 M KCl medium at holding potentials of −40 mV and +40 mV. With 50 μM Ca^{2+} in the *trans* chamber, the channels showed a typical behavior. Channel activities were higher at the negative potential and were characterized by long open events at −40 mV and short open events at +40 mV. Increase in [KCl] from 0.25 M to 0.5 M (second row) and 1.0 M (third row) decreased P_o and reduced the duration of the open events at −40 mV without appreciably affecting the two channel activities at +40 mV. The recordings in the fourth row show that a subsequent increase in lumenal [Ca^{2+}] (from 50 μM to 0.2 mM) resulted in an increase in P_o and the duration of the open events at −40 mV but not at +40 mV. In single-channel recordings, the two open time constants at −40 mV holding potential decreased from 0.74 ± 0.17 ms and 3.05 ± 0.72 ms to 0.29 ± 0.08 and 0.97 ± 0.17 ms (n = 5–12) as [KCl] was increased from 0.25 to 1.0 M. At 1.0 M KCl, as lumenal [Ca^{2+}] was raised to 0.2 mM, they increased to 0.89 ± 0.24 ms, 2.59 ± 0.69 ms (see Fig. 7 *B* for changes in P_o values). We calculated lumenal to cytosolic Ca^{2+} fluxes using ionic conditions comparable to those in Fig. 7 *A* and compared the calculated values with the channel activities of five separate recordings. Fig. 7 *B* shows that there existed an excellent correlation between measured channel activities and calculated Ca^{2+} fluxes.

Channel-mediated lumenal to cytosolic Ca^{2+} fluxes were also reduced by the addition of 1–5 mM $MgCl_2$ or 1–5 mM $BaCl_2$ to the *trans* chamber. Channels were initially recorded at −40 mV in symmetric 0.25 M KCl media with 50 μM lumenal Ca^{2+} and 45 nM cytosolic Ca^{2+} and 2 mM cytosolic ATP. Fig. 8 shows that the addition of 1 mM lumenal Mg^{2+} or 1 mM lumenal Ba^{2+} reduced the calculated Ca^{2+} flux about twofold (from 0.28 pA to 0.17 pA), but P_o was reduced more strongly from 0.3 to 0.08. An increase in lumenal [Mg^{2+}] or [Ba^{2+}] to 5 mM further decreased the calculated Ca^{2+} fluxes as well as channel activities. For comparative purposes, inhibition of channel activities and Ca^{2+} fluxes by increasing [KCl], already described in Fig. 7, is also shown in Fig. 8. Unlike [KCl], lumenal Mg^{2+} and Ba^{2+} had a higher potency in reducing

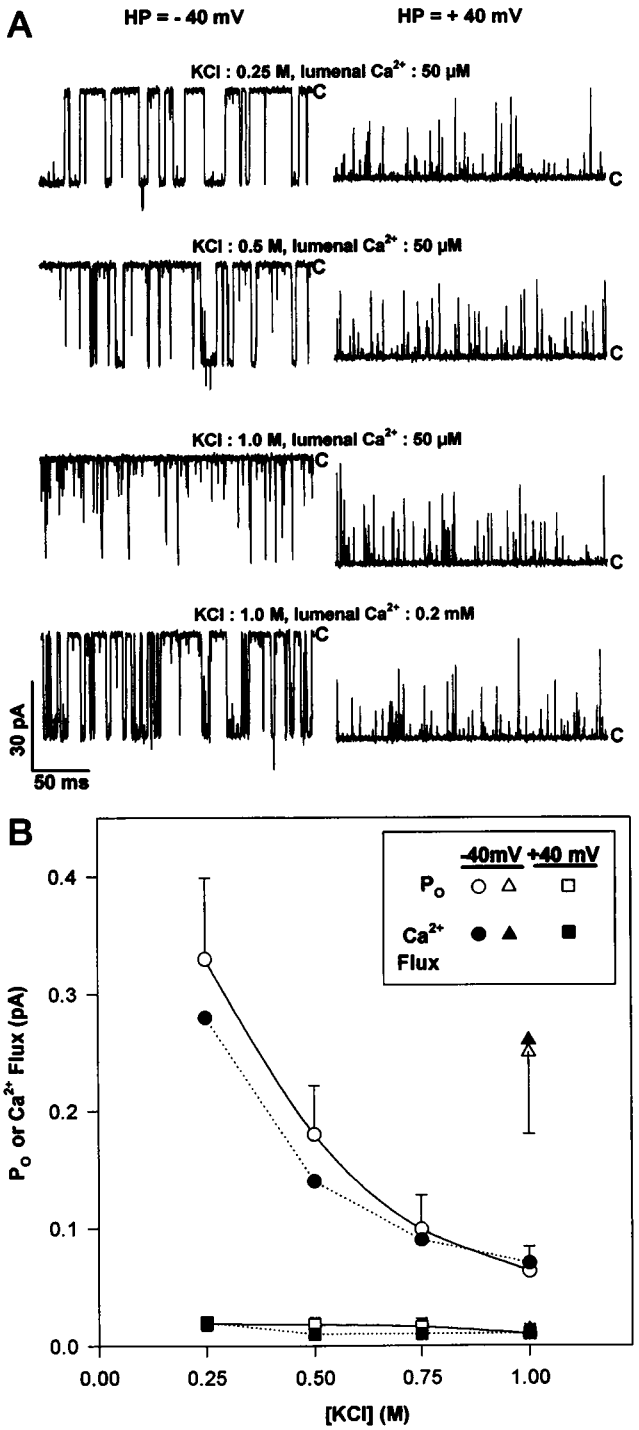

FIGURE 7 Effect of [KCl] on cytosolic ATP-, lumenal Ca^{2+}-activated channel activities and channel-mediated Ca^{2+} fluxes. All recordings are from a single experiment. (*A*) Recordings of two ATP-activated release channels at holding potentials of −40 mV (*left*) and +40 mV (*right*). Single-channel currents, shown as downward or upward deflections from the closed levels (marked C), were recorded in the following solutions. (*Top recordings*) *cis*, 0.25 M KCl, 10 mM KPIPES, pH 7.1, 2 mM ATP, 150 μM $CaCl_2$ and 2 mM EGTA (45 nM free Ca^{2+}); *trans*, 0.25 M KCl, 10 mM KPIPES, pH 7.1, 150 μM $CaCl_2$ and 100 μM EGTA (50 μM free Ca^{2+}). Left panel, P_o = 0.17; right panel, P_o = 0.002. (*Second recordings*) Solution composition as in top recordings, except that [KCl] was raised symmetrically to 0.5 M. Left panel, P_o = 0.12; right panel, P_o = 0.005. (*Third recordings*) Solution composition as in top and second recordings, except that [KCl] was raised symmetrically to 1.0 M. Left panel, P_o = 0.02; right panel, P_o = 0.005. (*Bottom recordings*) Solution composition as in third recordings, except that the lumenal free Ca^{2+} was raised to 0.2 mM (300 μM $CaCl_2$ + 100 μM EGTA). Left panel, P_o = 0.14; right panel, P_o = 0.006. (*B*) Mean P_o (○, △, □) from channels recorded as in *A* and calculated lumenal to cytosolic Ca^{2+} fluxes (●, ▲, ■) as a function of [KCl]. Holding potentials were −40 mV (○, △, ●, ▲) and +40 mV (□, ■). *Cis* free [Ca^{2+}] was 45 nM. Free *trans* [Ca^{2+}] was 50 μM (○, ●, □, ■) (n = 13) or 0.2 mM (△, ▲) (n = 6).

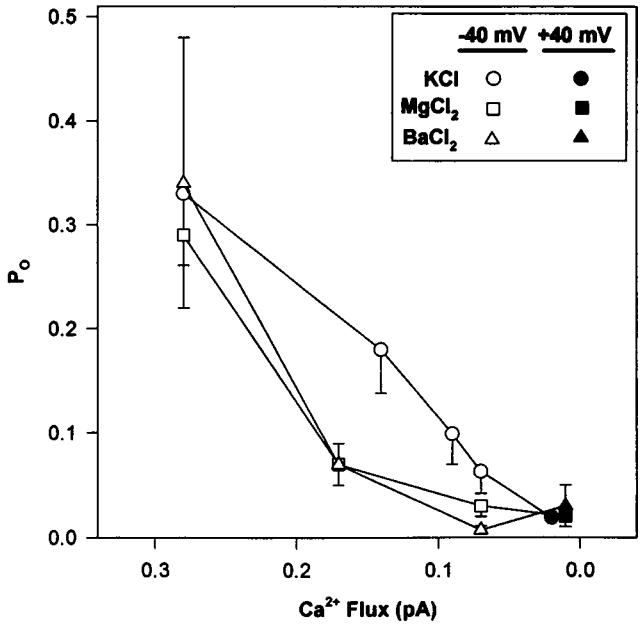

FIGURE 8 Effects of [KCl] and lumenal $MgCl_2$ and $BaCl_2$ on P_o and lumenal to cytosolic Ca^{2+} fluxes. Mean P_os were calculated from channel recordings at −40 mV (○, □, △) and +40 mV (●, ■, ▲) in 0.25 M KCl, 10 mM KPIPES, pH 7.1 media. The *cis* chamber solution contained 2 mM ATP, 150 μM $CaCl_2$, and 2 mM EGTA (45 nM free Ca^{2+}). The *trans* chamber solution contained 150 μM $CaCl_2$, 100 μM EGTA (50 μM free Ca^{2+}), and 0, 1, or 5 mM $MgCl_2$ or 0, 1, or 5 mM $BaCl_2$. Ca^{2+} fluxes were calculated as described in Materials and Methods. Data points are mean (± SE) of four experiments. Also shown are the mean P_o and calculated Ca^{2+} fluxes of channels, which were recorded as described in Fig. 6 at a constant lumenal [Ca^{2+}] of 50 μM and [KCl] of 0.25, 0.5, 0.75, and 1.0 M.

channel activities than Ca^{2+} fluxes. This result indicated that lumenal Ba^{2+} and Mg^{2+} reduced channel activity by some additional mechanism, possibly by having access to cytosolic Ca^{2+} activation and inhibition sites in addition to reducing Ca^{2+} fluxes.

Effects of the "fast" complexing Ca^{2+} buffer BAPTA

We considered the possibility that lumenal Ca^{2+} activates and inhibits the Ca^{2+} release channel (Figs. 4 and 5) by having access to both of the channel's Ca^{2+} activation and inhibition sites. We tested this idea using the "fast" complexing Ca^{2+} buffer 1,2-bis(2-aminophenoxy)ethanetetraacetic acid (BAPTA). Modeling studies have indicated that because of its high association rate BAPTA is much

more effective than the "slow" complexing Ca^{2+} buffer EGTA in suppressing a rise in Ca^{2+} concentration near the release sites (Stern, 1992). Cytosolic ATP-activated channel activities were recorded in the presence of 45 nM free cytosolic Ca^{2+} (150 μM Ca^{2+} and 2 mM EGTA) and 2 mM cytosolic ATP, and with either 50 μM or 10 mM free Ca^{2+} in the *trans* chamber. The addition of 10 mM cytosolic BAPTA increased (in three of four recordings) the activity of channels that were recorded under conditions that favored channel activation (50 μM lumenal Ca^{2+}, −40 mV; Fig. 4 *A*, *second recording*) (data not shown). This result suggested that the activating site(s) was (were) located in a "BAPTA-inaccessible" space but that BAPTA might have been able to complex Ca^{2+} before they could reach the inhibition site(s). BAPTA had no noticeable effect on channel conductance or when added to a <1 μM free lumenal Ca^{2+} solution.

The possibility that cytosolic BAPTA can remove lumenal Ca^{2+} flux-induced channel inhibition was examined in greater detail using a high lumenal [Ca^{2+}]. Fig. 9 *A* shows four current traces of a single ATP-activated channel that were recorded in the presence of 10 mM lumenal Ca^{2+} at −40 mV, i.e., under conditions that favored large lumenal to cytosolic Ca^{2+} fluxes. The top recording in Fig. 9 *A* shows that before the addition of BAPTA channel activity was relatively low (P_o = 0.05) in the presence of 2 mM cytosolic EGTA and 150 μM cytosolic Ca^{2+} (45 nM cytosolic Ca^{2+}). The second, third, and fourth recordings show a gradual increase in channel activity after the cytosolic addition of 10, 25, and 50 mM BAPTA, respectively. The P_o values at the different [BAPTA] were plotted against holding potentials of −60 mV to +60 mV (Fig. 9 *B*) and against the calculated lumenal to cytosolic Ca^{2+} fluxes (Fig. 9 *C*). The addition of 10 mM cytosolic BAPTA significantly increased P_o at holding potentials ranging from −60 mV to +40 mV. Additional significant increases in P_o were seen after the addition of 25 and 50 mM cytosolic BAPTA. The maximum increase in P_o was obtained at +20 mV, where the addition of 50 mM BAPTA increased the mean P_o from a control value of 0.26 ± 0.04 to 0.82 ± 0.07 (n = 5).

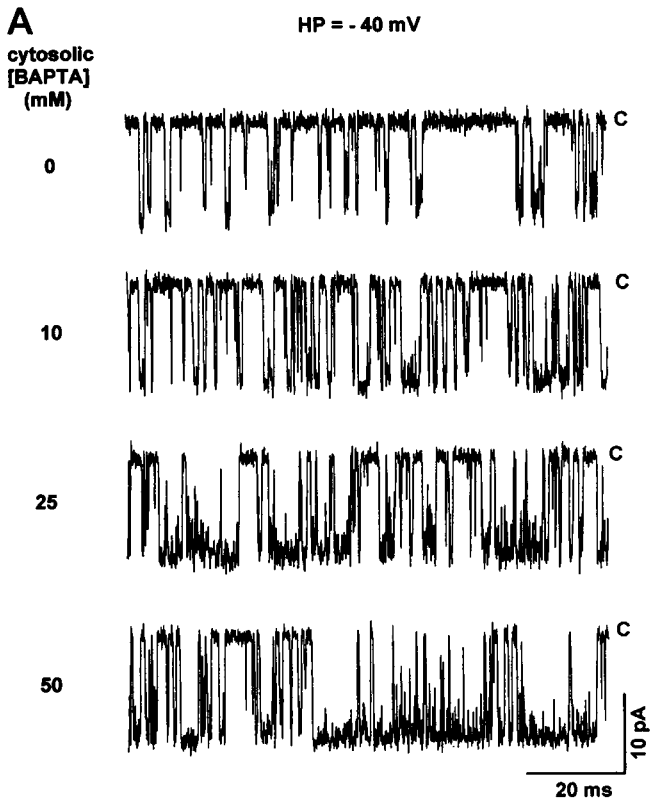

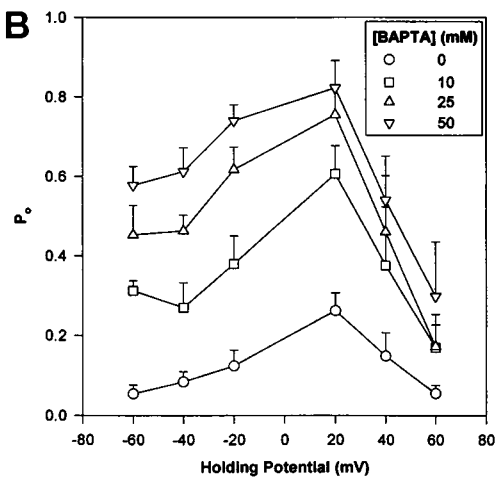

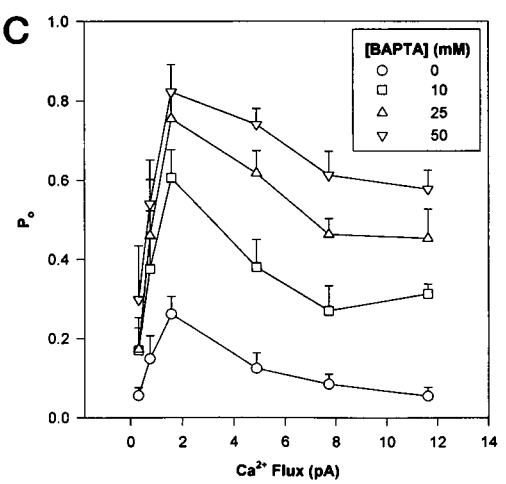

FIGURE 9 Effect of cytosolic BAPTA on cytosolic ATP-, lumenal Ca^{2+}-activated channel activities. (*A*) Single-channel currents, shown as downward deflections from closed levels (marked C), were recorded at −40 mV in symmetrical 250 mM KCl, 10 mM KPIPES, pH 7.1. The *trans* chamber solution contained 10.1 mM $CaCl_2$ and 100 μM EGTA (10 mM free Ca^{2+}). The *cis* chamber solution contained 2 mM ATP, 150 μM $CaCl_2$, 2 mM EGTA, and the indicated [BAPTA]: (*Top recording*) 0 mM BAPTA, P_o = 0.05. (*Second recording*) 10 mM BAPTA, P_o = 0.24. (*Third recording*) 25 mM BAPTA, P_o = 0.43. (*Bottom recording*) 50 mM BAPTA, P_o = 0.63. (*B, C*) Mean P_o values calculated from channel recordings as in *A* are plotted against holding potential (*B*) and against the calculated lumenal to cytosolic Ca^{2+} fluxes at holding potentials from −60 to +60 mV (*C*). Data are mean (±SE) of five experiments. Differences in P_o between 0 mM and 10, 25, and 50 mM BAPTA were significantly different at each voltage, except at +60 mV (in *B*) and at all Ca^{2+} fluxes except at 0.32 pA (Ca^{2+} flux at +60 mV) (in *C*). It should be noted that no data points were taken between 2 pA and 5 pA, as it was difficult to analyze Ca^{2+}-blocked K^+ currents near 0 mV.

Removal of channel inactivation by BAPTA increased the mean open times without significantly affecting the number of single-channel events. The mean open time constants at −40 mV holding potential increased from 0.52 ± 0.06 ms and 1.80 ± 0.38 ms before the addition of BAPTA to 1.22 ± 0.14 ms and 4.99 ± 0.31 ms after the addition of 50 mM BAPTA (n = 4). At +20 mV, the mean open time constants were 1.73 ± 0.41 and 5.80 ± 1.03 ms before the addition of BAPTA and 2.54 ± 0.49 and 17.55 ± 4.37 ms after the addition of 50 mM BAPTA (n = 4). Inspection of the P_o–Ca^{2+} flux relationships in Fig. 9 *C* suggested that the addition of cytosolic BAPTA resulted in a significant increase in channel activities at Ca^{2+} fluxes as low as ~0.75 pA (Ca^{2+} flux at +40 mV with 10 mM lumenal Ca^{2+} and nominally zero cytosolic Ca^{2+}). Channel activities also increased at a Ca^{2+} flux of less than 0.75 pA (at +60 mV), but these increases were not statistically significant. On the other hand, a cytosolic [BAPTA] as high as 50 mM was not sufficient to completely remove the inhibition that occurred at the high Ca^{2+} fluxes (i.e., at −40 and −60 mV). We conclude from these observations that high concentrations of BAPTA can, to a large extent, remove high Ca^{2+} flux-induced channel inhibition by complexing Ca^{2+} ions before they can reach the Ca^{2+} inactivation site(s), but that high BAPTA concentrations cannot prevent lumenal Ca^{2+} from reaching the Ca^{2+} activation site.

DISCUSSION

In the present study, we studied at the single-channel level the effects of SR lumenal Ca^{2+} on cytosolic ATP-activated Ca^{2+} release channels at low cytosolic [Ca^{2+}]. Our studies led to three novel observations regarding the mechanism of regulation of the channel by Ca^{2+} and adenine nucleotides. First, the data reported here provided insight into the action of adenine nucleotides by showing that at nanomolar lumenal and cytosolic [Ca^{2+}], ATP greatly increased the frequency of closed to open transitions. Second, our single-channel recordings showed that SR lumenal to cytosolic Ca^{2+} fluxes activated the ATP-activated channel by interacting with cytosolic Ca^{2+} activation sites. Third, our experiments with the "fast" Ca^{2+}-complexing buffer BAPTA showed that lumenal to cytosolic Ca^{2+} fluxes inhibited the skeletal muscle Ca^{2+} release channel by interacting with cytosolic Ca^{2+} inactivation sites.

Model of regulation of Ca^{2+} release channel by cytosolic ATP and lumenal Ca^{2+}

In this study, we examined the regulation of the ATP-activated skeletal muscle Ca^{2+} release channel by lumenal Ca^{2+} in the presence of a low cytosolic [Ca^{2+}]. Under our experimental conditions and according to the data of Table 1, the gating of the channel may be modeled as follows:

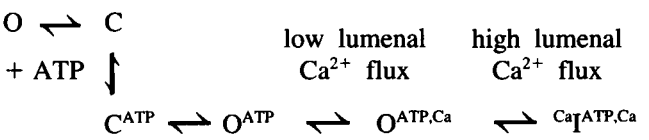

The above partial kinetic scheme has been simplified by showing for each experimental condition only one of the two open states (Table 1). Similarly, it is likely that there are more than one closed (or inactivated) state for each condition indicated above. The scheme proposes that the Ca^{2+} release channel is present in (i) ligand-free closed state(s) (C) and infrequently occurring open state(s) (O) in the absence of ATP at cytosolic and lumenal [Ca^{2+}] of <0.1 μM; (ii) ATP-liganded closed (C^{ATP}) and open (O^{ATP}) states in the presence of 2 mM ATP and cytosolic and lumenal [Ca^{2+}] <0.1 μM; (iii) ATP-liganded, Ca^{2+}-activated states ($O^{ATP,Ca}$) in the presence of 2 mM ATP and a low lumenal to cytosolic Ca^{2+} flux; and (iv) ATP-liganded, Ca^{2+}-inactivated states ($^{Ca}I^{ATP,Ca}$) in the presence of 2 mM ATP and a high lumenal to cytosolic Ca^{2+} flux. Below we shall first describe the scheme before addressing the question of the location of the Ca^{2+} regulatory sites and discussing the physiological implications of our results.

Activation by ATP

Vesicle-ion flux studies have shown that the skeletal muscle Ca^{2+} release channel can be activated by micromolar [Ca^{2+}] or millimolar [ATP], but can be optimally activated only by the combined presence of Ca^{2+} and ATP to give maximum Ca^{2+} release rates with first-order rate constants of 20–100 s^{-1} (Meissner, 1994). In single-channel measurements, millimolar ATP in the presence of micromolar cytosolic Ca^{2+} and millimolar (Smith et al., 1986) or nanomolar (this study) lumenal Ca^{2+} has been shown to greatly activate the channel and to increase the channel open time constants. As observed in this study, Sitsapesan and Williams (1995) found that channel activities could also be markedly increased by ATP at low cytosolic [Ca^{2+}] when lumenal [Ca^{2+}] was raised to high micromolar to millimolar Ca^{2+} concentrations. At variance with our interpretation of these data (see below), these authors suggested that the effects of lumenal Ca^{2+} were most likely mediated by specific Ca^{2+} binding sites on the lumenal face of the channel and that these sites were exposed only when cytosolic ATP bound to the channel. Sitsapesan and Williams (1995) furthermore observed that channels activated by ATP ceased to open when the Ca^{2+} concentrations at both sides of the bilayer were reduced to picomolar levels. In our experiments, Ca^{2+} release channels rarely opened in the presence of low levels of Ca^{2+} and in the absence of ATP. However, in contrast to Sitsapesan and Williams (1995), we observed frequent but short channel openings when channel activities were recorded at picomolar levels of Ca^{2+} in the presence of 2 mM cytosolic ATP. In the above scheme, these observations are taken into account by proposing that

the ligand-free Ca^{2+} release channel opens only occasionally for brief periods but that the transition rate from the closed to open states is greatly accelerated by the occupation of the channel's ATP binding site(s) (Table 1).

Activation of ATP-activated channel by lumenal Ca^{2+}

Activation of the Ca^{2+} release channel by lumenal Ca^{2+} was analyzed in the presence of cytosolic ATP at subactivating levels of cytosolic Ca^{2+}. Lumenal to cytosolic Ca^{2+} fluxes were estimated to determine if there was a direct correlation between channel activity and channel-mediated Ca^{2+} fluxes. In estimating the Ca^{2+} fluxes, we relied on the four-barrier, three-binding site model of Tinker et al. (1992, 1993) because we found that this model, developed for the sheep cardiac channel, could also be used to approximate the individual ionic fluxes of the rabbit skeletal muscle release channel in solutions containing K^+ and Ca^{2+} as conducting ions. A reasonably linear relationship between P_o and Ca^{2+} fluxes was obtained at low Ca^{2+} fluxes (<1.5 pA; Fig. 5 *C*) at different lumenal [Ca^{2+}] and holding potentials. The most straightforward explanation of these results is that Ca^{2+} flowing through the channel pore activated the channel by binding to cytosolic Ca^{2+} activation sites. The observation that lumenal to cytosolic Ca^{2+} fluxes primarily activated the channel by increasing the duration of the channel openings suggested that a greater occupancy of the Ca^{2+} activation sites decreased the transition rates from the open to closed channel states. Appearance of open events with longer durations appeared to depend on the presence of ATP, because open events with a duration greater than 1 ms were rarely seen with Ca^{2+} as the sole activating ligand (Table 1).

In the study by Sitsapesan and Williams (1995), lumenal Ca^{2+} increased the activity of skeletal muscle Ca^{2+} release channels that were activated by ATP or ATP and cytosolic Ca^{2+} but not by cytosolic Ca^{2+} alone. This result excluded, according to the authors, "the possibility that lumenal Ca^{2+} flowing through the channel has direct access to the cytosolic Ca^{2+}-activation site/s." In contrast, in our experiments lumenal to cytosolic Ca^{2+} fluxes increased the activity of channels that were solely activated by submicromolar concentrations of Ca^{2+} (Fig. 6). The major effect of lumenal Ca^{2+} was to increase the mean duration of the open events. A 1.4-fold (not significant) increase in the number of channel events was also seen. Cytosolic Ca^{2+} increased channel activity by predominantly increasing the frequency of channel openings and closings (Smith et al., 1986; Sitsapesan et al., 1995; Table 1). If the lumenal to cytosolic Ca^{2+} flux has access to the cytosolic Ca^{2+} activation site(s), then why do we not see a major effect on the frequency of channel openings as well? One possible explanation is that cytosolic Ca^{2+} is always available to bind to the cytosolic Ca^{2+} activation site(s); however, this may not be the case with the lumenal Ca^{2+} flux. When the channel opens, lumenal Ca^{2+} can flow toward the cytosol, and a steady-state concentration of Ca^{2+} can rapidly build up near the mouth of the pore (Simon and Llinas, 1985). But once the channel closes, the Ca^{2+} gradient at the cytosolic side of the channel would dissipate very rapidly, and rebinding of Ca^{2+} to the Ca^{2+} activation site(s) would be much less likely. Thus, it is not unreasonable to see an increase in open duration but only a small increase in opening frequency by lumenal to cytosolic Ca^{2+} fluxes. We conclude that even in the absence of ATP, lumenal Ca^{2+} can reach cytosolic Ca^{2+} activation sites.

We did not observe a significant decrease in P_o when lumenal Ca^{2+} was varied from 45 nM to 50 μM at an optimal (50 μM) cytosolic Ca^{2+} (Table 1). Under these recording conditions, there occurs only a small increase in lumenal to cytosolic Ca^{2+} flux (a flux of ~0.25 pA at −40 mV was calculated using the model of Tinker et al., 1992, 1993). Such a small flux appears to be insufficient to cause channel inhibition (Fig. 5 *C*). However, we predict that a decrease in P_o would occur when the lumenal [Ca^{2+}] is raised to millimolar levels. Indeed, in two (out of two) experiments, the P_o at −40 mV holding potential decreased ~3-fold and ~5-fold when lumenal [Ca^{2+}] was raised from 50 μM to 1 and 5 mM, respectively (data not shown). Under the above recording conditions, the model would predict a large lumenal to cytosolic Ca^{2+} flux of ~3.5 and ~6.8 pA, respectively.

In support of a direct access of lumenal Ca^{2+} to cytosolic Ca^{2+} activation sites were our observations that P_o and open time constants decreased when the lumenal to cytosolic Ca^{2+} fluxes were reduced by an increase in [KCl] from 0.25 M to 1.0 M or by the addition of 1–5 mM lumenal Mg^{2+} or Ba^{2+} (Figs. 7 and 8). The effects of increasing [KCl] were not due to any nonspecific effects, as increased channel activity and long open events reappeared at 1.0 M symmetrical KCl when lumenal to cytosolic Ca^{2+} fluxes were increased by raising lumenal Ca^{2+} from 50 μM to 0.2 mM (Fig. 7). The two divalent cations were more effective in decreasing channel activity than the increases in [KCl]. In addition to reducing the Ca^{2+} flux, Ba^{2+} and Mg^{2+} may have inhibited Ca^{2+} release channel activity by binding to high-affinity cytosolic Ca^{2+} activation and/or low-affinity cytosolic Ca^{2+} inactivation sites (Meissner, 1994). In support of this suggestion, the ionic flux calculations using the four-barrier, three-ion binding model of Tinker et al. (1992, 1993) showed that in the presence of 1 and 5 mM lumenal Mg^{2+} (or Ba^{2+}), there was a large lumenal to cytosolic Mg^{2+} (or Ba^{2+}) flux of ~2.5 and ~5 pA, respectively.

Inactivation of ATP-activated channel by lumenal Ca^{2+}

An increase in the lumenal Ca^{2+} fluxes from 0 to ~1.25 pA led to an increase in ATP-activated channel activity. Channel activity was at a maximum at an estimated Ca^{2+} flux of

~1.25 pA and declined slowly as the Ca^{2+} fluxes increased further (Fig. 5 *C*). One possible explanation of these results was that a Ca^{2+} flux of ~1.25 pA was sufficient to maximally occupy the cytosolic Ca^{2+} activation sites. However, arguing against such a mechanism is the fact that the maximum channel activities observed under our standard recording conditions (P_o ~ 0.4; Fig. 5) were appreciably lower than those we obtained for channels that were activated by 2 mM cytosolic ATP and 5–10 μM cytosolic Ca^{2+} (P_o ~ 0.9) (Fig. 2 *B*). Another possibility we considered therefore was that lumenal Ca^{2+} could not maximally activate the channel because it could reach Ca^{2+} inactivation sites, in addition to the Ca^{2+} activation sites. In support of a direct access to cytosolic Ca^{2+} inactivation sites, we found that the cytosolic addition of the fast Ca^{2+}-complexing buffer BAPTA increased P_o close to a maximum value (P_o ~ 0.8). Therefore, high concentrations of BAPTA were apparently able to remove lumenal Ca^{2+}-induced channel inhibition by minimizing the built-up of a high cytosolic Ca^{2+} concentration gradient at the inactivation site(s). Our observation that BAPTA did not prevent channel activation but could remove high lumenal to cytosolic Ca^{2+} flux-induced channel inactivation suggested that the Ca^{2+} activation and Ca^{2+} inactivation sites were located in "BAPTA-inaccessible" and "BAPTA-accessible" spaces, respectively. Some possible reasons for the BAPTA inaccessibility of the Ca^{2+} activation sites could be that they are located within the loosely packed "foot" region of the channel at sites that are accessible to Ca^{2+} but not to BAPTA, because of steric reasons or dominant fixed charges. BAPTA had no noticeable effect when ATP-activated channel activity was low because of a low Ca^{2+} flux (data not shown). A direct pharmacological activation of the channel by BAPTA appeared therefore to be unlikely.

Location of cytosolic Ca^{2+} activation and Ca^{2+} inactivation sites

Electron microscopic and imaging studies have indicated that the skeletal muscle Ca^{2+} release channel consists of a large, loosely packed cytosolic assembly with overall dimensions of 29 × 29 × 12 nm and a smaller transmembrane assembly that extends ~7 nm toward the SR lumen and likely contains the Ca^{2+} channel pore (Radermacher et al., 1994; Serysheva et al., 1995). The path(s) of Ca^{2+} to reach the myoplasm as it emerges from the conductance pore is (are) not precisely known. In the reconstruction of Radermacher et al. (1994) the top surface of the cytoplasmic domain is open at its center. However, the cytoplasmic end of the transmembrane Ca^{2+} conducting pathway appeared to be "plugged" by a globular mass of density, and four radially running channels could be discerned on the sides of the transmembrane assembly near its junction with the cytoplasmic assembly. These pathways have been hypothesized to be exit pathways for Ca^{2+}. In the reconstruction of Serysheva et al. (1995) the top view of the cytoplasmic assembly shows a central opening of ~5 nm, and no radial channels are evident. Thus it is possible there exist a number of exit pathways for Ca^{2+} as it emerges from the channel pore.

We considered the possibility that the Ca^{2+} activation site(s) of the Ca^{2+} release channel lies in the ion conductance pathway. We calculated the apparent K_d for the Ca^{2+} binding site (located in the membrane electric field) following the procedure of Tinker et al. (1993). The calculated values at holding potentials of +40 and −40 mV with different lumenal [Ca^{2+}] were in the millimolar range. This is much higher than the K_m for the cytosolic activation site, which was in the presence of ATP in the low micromolar range (Fig. 2 *B*). Furthermore, no differences in channel activity were observed at +40 and −40 mV in our experiments, which were done at nanomolar lumenal Ca^{2+} and 2 mM cytosolic ATP and varying cytosolic [Ca^{2+}] (Fig. 2). A simple calculation assuming a K_m of 2×10^{-6} M (calculated from Fig. 2 *B*), $k_1 = k_{-2} = 10^9\ M^{-1}\ s^{-1}$, $k_{-1} = k_2 = 2 \times 10^3\ s^{-1}$, and $\delta = 0.5$ (where k_1 and k_{-2} are the rate constants of Ca^{2+} entry at 0 mV from cytosolic and lumenal sides, respectively, to a binding site located at an electrical distance δ of 0.5 from the lumenal side, and k_{-1} and k_2 are the rate constants of Ca^{2+} ions leaving the site at 0 mV to the cytosolic and lumenal sides, respectively) predicts a ~4-fold higher occupancy at +40 mV compared to that at −40 mV at a cytosolic [Ca^{2+}] of 0.5 μM and a ~3-fold higher occupancy at a cytosolic [Ca^{2+}] of 2.5 μM. However, the channel activities were very similar at the two holding potentials at the above cytosolic Ca^{2+} concentrations. The calculated differences in occupancy were higher when the binding site was moved closer to the lumenal side, and lower when the site was moved closer to the cytosolic side. A ~4-fold lower occupancy was calculated assuming a cytosolic location of the site ($\delta = 1$) at a cytosolic [Ca^{2+}] of 0.5 μM. The occupancy at +40 mV was similar to that at −40 mV at a δ of 0.75. Similar calculations assuming a δ of 0.75 predicted a ~1.5-fold and ~1.1-fold higher occupancy at −40 mV compared to that at +40 mV at a lumenal [Ca^{2+}] of 50 μM and 250 μM, respectively, with nominally zero cytosolic [Ca^{2+}]. However, the mean P_o was 7-fold and 9-fold higher at −40 mV compared to that at +40 mV at the above two lumenal [Ca^{2+}], respectively (Table 1). Therefore, we considered it unlikely that the Ca^{2+} activation site(s) of the Ca^{2+} release channel lies in the ion conductance pathway.

Of particular interest was our observation that ATP-activated channels could be nearly maximally activated by lumenal Ca^{2+} when the *cis* chamber of the bilayer apparatus contained 50 mM BAPTA but could not be activated more than half-maximally when the only Ca^{2+} chelator present was 2 mM EGTA. The free cytosolic Ca^{2+} concentration gradient formed by the lumenal Ca^{2+} fluxes was calculated according to Stern (1992). A simple expression derived by him (equation 13 of his paper) was used which yields the free Ca^{2+} concentration as a function of distance, if the rate of Ca^{2+} flux through the channel and the initial concentra-

tions of total and uncomplexed Ca^{2+} and Ca^{2+} buffer are known. The following constants were used for Ca^{2+} and EGTA: $k_{on} = 2.5 \times 10^6\ M^{-1}\ s^{-1}$; $K_d = 1.6 \times 10^{-7}$ M, $D_{Ca} = 3 \times 10^{-6}\ cm^2\ s^{-1}$, $D_{EGTA} = D_{CaEGTA} = 10^{-5}\ cm^2\ s^{-1}$. If we assume a single cytosolic Ca^{2+} exit pathway and a cytosolic [EGTA] of 2 mM, we calculate that a lumenal Ca^{2+} flux as small as 0.01 pA (a value obtained at +40 mV holding potential with a lumenal [Ca^{2+}] of 50 μM and nanomolar cytosolic Ca^{2+}, using the model of Tinker et al., 1992, 1993) would result in a [Ca^{2+}] of 5 μM and 10 μM, respectively, at a distance of ~5 nm and 2.5 nm from the Ca^{2+} exit site. Such close proximity of the Ca^{2+} activation sites to the Ca^{2+} exit site should have led to a nearly maximum channel activity (Fig. 2) as cytosolic [Ca^{2+}] of 5 and 10 μM nearly fully activated the Ca^{2+} release channel in the presence of 2 mM ATP. Clearly this was not the case, as at a lumenal Ca^{2+} flux of 0.01 pA only low channel activities (P_o ~0.03) were observed (Fig. 5 *C*). A P_o of 0.03 was estimated at a cytosolic [Ca^{2+}] of 0.25 μM in the presence of 2 mM ATP (Fig. 2 *B*). A further calculation using Stern's equation (Stern, 1992) as outlined with 2 mM EGTA and a Ca^{2+} flux of 0.01 pA predicted that a distance of ~75 nm from the Ca^{2+} exit site was required to lower [Ca^{2+}] to 0.25 μM. This distance is much larger than the dimensions of the skeletal muscle RyR (Radermacher et al., 1994; Serysheva et al., 1995). The apparent paradox between the measured and calculated effects of lumenal [Ca^{2+}] suggested that the Ca^{2+} activation sites are located within the loosely packed "foot" region of the channel at sites that are more readily accessible to cytosolic Ca^{2+} than to lumenal Ca^{2+} fluxes. One possibility is that the four putative radially running channels located in the cytoplasmic portion of the channel (Radermacher et al., 1994) have a role in carrying a small portion of the total lumenal Ca^{2+} flux to the Ca^{2+} activation sites. The Ca^{2+} activation sites could be inaccessible to BAPTA because of kinetic (if the sites are close to the exit sites), steric, or electrostatic reasons. If the Ca^{2+} activation sites see a minor portion and the Ca^{2+} inactivation sites see a major portion of the lumenal Ca^{2+}, increases in lumenal [Ca^{2+}] would result in a smaller increase in [Ca^{2+}] near the Ca^{2+} activation sites and a larger increase in [Ca^{2+}] near the Ca^{2+} inactivation sites. In such a case, as observed in the present study, Ca^{2+} inactivation will take place before the channel can be fully activated by lumenal Ca^{2+}.

The distance between the channel pore and cytosolic Ca^{2+} inactivation site(s) was estimated assuming that the inactivation site(s) lies near a single major Ca^{2+} exit site (the central opening of the channel; Serysheva et al., 1995) and that a cytosolic [Ca^{2+}] of 100–250 μM was sufficient to cause channel inactivation (Meissner, 1994). The free Ca^{2+} concentration gradient near the central opening as a function of distance was calculated according to the method of Stern (1992). In our experiments (Fig. 9 *C*), the addition of 50 mM BAPTA resulted in a significant increase of channel activity at a Ca^{2+} flux of ~0.75 pA. The distance from the Ca^{2+} exit site at which 50 mM BAPTA can reduce the Ca^{2+} concentration to a level of 100–250 μM at a Ca^{2+} flux of 0.75 pA was calculated to be ~3 nm. This distance was calculated using the following constants for Ca^{2+} and BAPTA: $k_{on} = 1.7 \times 10^9\ M^{-1}\ s^{-1}$; $K_d = 4 \times 10^{-7}$ M, $D_{Ca} = 3 \times 10^{-6}\ cm^2\ s^{-1}$, $D_{BAPTA} = D_{CaBAPTA} = 10^{-5}\ cm^2\ s^{-1}$. Thus we estimate a lower limit of ~3 nm for the distance between the cytosolic Ca^{2+} inactivation site(s) and the Ca^{2+} exit site. A distance of ~6 nm was calculated at a Ca^{2+} flux of ~12 pA (Ca^{2+} flux at 10 mM lumenal Ca^{2+} and −60 mV holding potential). Because at a lumenal Ca^{2+} flux of ~12 pA, 50 mM BAPTA did not completely remove high Ca^{2+} flux-induced channel inhibition (Fig. 9 *C*), we would place the inactivation site at a distance closer than 6 nm but more distant than 3 nm from the Ca^{2+} exit site. At variance with our conclusion, Fill et al. (1990) envisioned the inactivation site occupying the interior of the ion conduction pathway, as it was accessible from both sides of the SR membrane.

Physiological implications

A characteristic feature of vertebrate skeletal muscle excitation-contraction (E-C) coupling is that it can occur in the absence of extracellular Ca^{2+}. This finding led to the formulation of the "mechanical coupling" mechanism, which suggests that voltage-sensing transverse tubule (T-tubule) dihydropyridine receptors (DHPR)/Ca^{2+} channels open SR Ca^{2+} release channels through direct protein-protein interactions. However, more recent studies have suggested that vertebrate skeletal muscle E-C coupling is regulated, in addition to DHPR-dependent mechanisms, by Ca^{2+}-dependent mechanisms (for reviews, see Rios and Pizarro, 1991; Schneider, 1994). Morphological evidence has suggested that in skeletal muscle some, but not all, SR Ca^{2+} release channels are linked to groups of four T-tubule particles presumed to represent four DHPRs (for a review, see Franzini-Armstrong and Jorgensen, 1994). This finding has led to the view that Ca^{2+} are initially released in response to a muscle action potential by SR Ca^{2+} release channels that are coupled to DHPRs. Studies with intact and cut fibers, muscle homogenates, and isolated triads using the fast Ca^{2+}-complexing buffers BAPTA and/or fura-2 have suggested that in skeletal muscle the released Ca^{2+} may both activate and inactivate further SR Ca^{2+} release. In rabbit skeletal muscle homogenates, a large T-tubule depolarization-induced, Ca^{2+}-dependent SR Ca^{2+} release could be abolished by ≥4 mM BAPTA (Anderson and Meissner, 1995). In studies with isolated triads, BAPTA also suppressed a secondary Ca^{2+}-dependent Ca^{2+} release component (Yano et al., 1995). Microinjection of millimolar [BAPTA] or [fura-2] into intact frog muscle fibers resulted in the disappearance of an early Ca^{2+} release component, which suggested that the early Ca^{2+} release component was activated by Ca^{2+} (Jacquemond et al., 1991). Other investigators found that the

injection of intermediate concentrations of fast Ca^{2+}-complexing buffers into intact fibers increased the rate and amount of Ca^{2+} release during an action potential (Hollingworth et al., 1992; Pape et al., 1993; Jong et al., 1993). These results suggested that Ca^{2+}-induced inactivation was removed, resulting in higher Ca^{2+} release. Vesicle-ion flux and single-channel measurements have shown that cytosolic Ca^{2+} regulates SR Ca^{2+} release channel activity by binding to high-affinity Ca^{2+} activation and low-affinity Ca^{2+} inactivation sites (Meissner, 1994). One important question that was not resolved in the above-cited studies was whether the released Ca^{2+} can regulate SR Ca^{2+} release by binding to the same channel. The results of our single-channel experiments demonstrated that Ca^{2+} flowing through a Ca^{2+} release channel can control SR Ca^{2+} release by binding to cytosolic Ca^{2+} activation and Ca^{2+} inactivation sites on the same channel. Furthermore, our studies indicated that lumenal to cytosolic Ca^{2+} fluxes inactivate the Ca^{2+} release channels before fully activating them, and that Ca^{2+} inactivation could be removed by high concentrations of BAPTA added to the cytosolic side. Other mechanisms that may activate and reduce SR Ca^{2+} release are calmodulin activation and inhibition of Ca^{2+} release channel activity (Tripathy et al., 1995), SR Ca^{2+} depletion (Baylor and Hollingworth, 1988), and Ca^{2+} release channel adaptation (Gyorke et al., 1994).

Ion flux-induced activation and inactivation of ion channels are not uncommon mechanisms of regulating intracellular processes. Examples are calcium-induced calcium release in cardiac muscle involving activation of the SR Ca^{2+} release channel by a surface membrane Ca^{2+} channel (Fabiato, 1985; Nabauer et al. 1989), and Ca^{2+}-dependent activation of Cl^- channels and K^+ channels (Hille, 1991). For the voltage-dependent *Torpedo* Cl^- channel, a self-amplification by the permeant Cl^- was recently described (Pusch et al., 1995). Ca^{2+} influx-dependent inactivation of surface membrane Ca^{2+} channels has been demonstrated in many cell types throughout the animal kingdom (Hille, 1991; Zong et al., 1994). Our results show that the permeant Ca^{2+} can both activate and inactivate the skeletal muscle Ca^{2+} release channel by having direct access to cytosolic Ca^{2+} activation and Ca^{2+} inactivation sites.

The authors thank Dr. Alan J. Williams for the computer program used to calculate the lumenal to cytosolic Ca^{2+} fluxes, and Dr. Judy Heiny for the computer program in estimating the Ca^{2+} gradient near the Ca^{2+} release sites. The latter program is based on equation 13 of the paper by Stern (1992).

This work was supported by a grant from the National Institutes of Health (AR18687).

REFERENCES

Anderson, K., and G. Meissner. 1995. T-tubule depolarization-induced SR Ca^{2+} release is controlled by dihydropyridine receptor- and Ca^{2+}-dependent mechanisms in cell homogenates from rabbit skeletal muscle. *J. Gen. Physiol.* 105:363–383.

Baylor, S. M., and S. Hollingworth. 1988. Fura-2 calcium transients in frog skeletal muscle fibers. *J. Physiol.* 403:151–192.

Colquhoun, D., and F. J. Sigworth. 1983. Fitting and statistical analysis of single-channel recording. *In* Single-Channel Recording. B. Sakmann and E. Neher, editors. Plenum Press, New York. 191–263.

Donoso, P., H. Prieto, and C. Hidalgo. 1995. Luminal calcium regulates calcium release in triads isolated from frog and rabbit skeletal muscle. *Biophys. J.* 68:507–515.

Fabiato, A. 1985. Time and calcium dependence of activation and inactivation of calcium-induced release of calcium from the sarcoplasmic reticulum of a skinned canine cardiac Purkinje cell. *J. Gen. Physiol.* 85:247–289.

Fill, M., R. Coronado, J. R. Mickelson, J. Vilven, J. Ma, B. A. Jacobson, and C. F. Louis. 1990. Abnormal ryanodine receptor channels in malignant hyperthermia. *Biophys. J.* 50:471–475.

Franzini-Armstrong, C., and A. O. Jorgensen. 1994. Structure and development of E-C coupling units in skeletal muscle. *Annu. Rev. Physiol.* 56:509–534.

Gyorke, S., P. Velez, B. Suarez-Isla, and M. Fill. 1994. Activation of single cardiac and skeletal ryanodine receptor channels by flash photolysis of caged Ca^{2+}. *Biophys. J.* 66:1879–1886.

Hille, B. 1991. Potassium channels and chloride channels, and calcium channels. *In* Ionic Channels of Excitable Membranes. Sinauer, Sunderland, MA. 115–139.

Hollingworth, S., A. B. Harkins, N. Kurebayashi, M. Konishi, and S. M. Baylor. 1992. Excitation-contraction coupling in intact frog skeletal muscle fibers injected with mmolar concentrations of fura-2. *Biophys. J.* 63:224–234.

Jacquemond, V., L. Csernoch, M. G. Klein, and M. F. Schneider. 1991. Voltage-gated and calcium-gated release during depolarization of skeletal muscle fibers. *Biophys. J.* 60:867–873.

Jong, D. S., P. C. Pape, W. K. Chandler, and S. M. Baylor. 1993. Reduction of calcium inactivation of sarcoplasmic reticulum calcium release by fura-2 in voltage-clamped cut twitch fibers from frog muscle. *J. Gen. Physiol.* 102:333–370.

Lee, H-B., L. Xu, and G. Meissner. 1994. Reconstitution of the skeletal muscle ryanodine receptor-Ca^{2+} release channel protein complex into proteoliposomes. *J. Biol. Chem.* 269:13305–13312.

Ma, J., M. Fill, C. M. Knudson, K. P. Campbell, and R. Coronado. 1988. Ryanodine receptor of skeletal muscle is a gap junction-type channel. *Science.* 242:99–102.

Meissner, G. 1984. Adenine nucleotide stimulation of Ca^{2+}-induced Ca^{2+} release in sarcoplasmic reticulum. *J. Biol. Chem.* 259:2365–2374.

Meissner, G., E. Darling, and J. Eveleth. 1986. Kinetics of rapid Ca^{2+}release by sarcoplasmic reticulum. Effects of Ca^{2+}, Mg^{2+} and adenine nucleotides. *Biochemistry.* 25:236–244.

Meissner, G. 1994. Ryanodine receptor/Ca^{2+} release channels and their regulation by endogenous effectors. *Annu. Rev. Physiol.* 56:485–508.

Nabauer, M., G. Callewaert, L. Cleemann, and M. Morad. 1989. Regulation of calcium release is gated by calcium current, not gating charge, in cardiac myocytes. *Science.* 244:800–803.

Pape, P. C., D. S. Jong, W. K. Chandler, and S. M. Baylor. 1993. Effect of fura-2 on action potential-stimulated calcium release in cut twitch fibers from frog muscle. *J. Gen. Physiol.* 102:295–332.

Pusch, M., U. Ludewig, A. Rehfeldt, and T. J. Jentsch. 1995. Gating of the voltage-dependent chloride channel ClC-0 by the permeant anion. *Nature.* 373:527–531.

Radermacher, M., V. Rao, R. Grassucci, J. Frank, A. P. Timerman, S. Fleischer, and T. Wagenknecht. 1994. Cryo-electron microscopy and three-dimensional reconstruction of the calcium release channel/ryanodine receptor from skeletal muscle. *J. Cell Biol.* 127:411–423.

Rios, E., and G. Pizzaro. 1991. Voltage sensor of excitation-contraction coupling in skeletal muscle. *Physiol. Rev.* 71:849–908.

Sachs, F., J. Neil, and N. Barkakati. 1982. The automated analysis of data from single ionic channels. *Pflugers Arch.* 395:331

Schneider, M. F. 1994. Control of calcium release in functioning skeletal muscle fibers. *Annu. Rev. Physiol.* 56:463–484.

Schoenmakers, J. M., G. J. Visser, G. Flick, and A. P. R. Theuvene. 1992. CHELATOR: an improved method for computing metal ion concentrations in physiological solutions. *Biotechniques.* 12:870–879.

Serysheva, I. I., E. V. Orlova, W. Chiu, M. B. Sherman, S. L. Hamilton, and M. van Heel. 1995. Electron cryomicroscopy and angular reconstitution used to visualize the skeletal muscle calcium release channel. *Nature Struct. Biol.* 2:18–24.

Simon, S. M., and Llinas, R. R. 1985. Compartmentalization of the submembrane calcium activity during calcium influx and its significance in transmitter release. *Biophys. J.* 48:485–498.

Sitsapesan, R., and A. J. Williams. 1995. The gating of the sheep skeletal sarcoplasmic reticulum Ca^{2+}-release channel is regulated by luminal Ca^{2+}. *J. Membr. Biol.* 146:133–144.

Smith, J. S., R. Coronado, and G. Meissner. 1986. Single-channel measurements of the calcium release channel from the sarcoplasmic reticulum: activation by Ca^{2+} and ATP and modulation by Mg^{2+}. *J. Gen. Physiol.* 88:573–588.

Stern, M. D. 1992. Buffering of calcium in the vicinity of a channel pore. *Cell Calcium.* 13:183–192.

Tinker, A., A. R. G. Lindsay, and A. J. Williams. 1992. A model for ionic conduction in the ryanodine receptor-channel of sheep cardiac muscle sarcoplasmic reticulum. *J. Gen. Physiol.* 100:495–517.

Tinker, A., A. R. G. Lindsay, and A. J. Williams. 1993. Cation conduction in the calcium release channel of the cardiac sarcoplasmic reticulum under physiological and pathophysiological conditions. *Cardiovasc. Res.* 27:1820–1825.

Tripathy, A., and G. Meissner. 1995. Evidence for a Ca^{2+}-activating site in or near the conduction pathway of the skeletal muscle Ca^{2+} release channel. *Biophys. J.* 68:A356.

Tripathy, A., L. Xu, and G. Meissner. 1995. Calmodulin activation and inhibition of skeletal muscle Ca^{2+} release channel. *Biophys. J.* 69:106–119.

Xu, L., R. Jones, and G. Meissner. 1993. Effects of local anesthetics on single channel behavior of skeletal muscle calcium release channel. *J. Gen. Physiol.* 101:207–233.

Yano, M., R. El-Hayek, and N. Ikemoto. 1995. Role of calcium feedback in excitation-contraction coupling in isolated triads. *J. Biol. Chem.* 270:19936–19942.

Zong, S., J. Zhou, and T. Tanabe. 1994. Molecular determinants of calcium-dependent inactivation of cardiac L-type calcium channels. *Biochem. Biophys. Res. Commun.* 201:1117–1123.